ISAS - INTERNATIONAL SCHOOL FOR ADVANCED STUDIES

Thesis submitted for the degree

of

"MAGISTER PHILOSOPHIAE"

Fe II EMISSION LINES in AGNs

Candidate

CRISTINA MARSI

Supervisor

Dr. P.L. SELVELLI

Academic Year 1986/87

TRIESTE

ISSA - SCUOLA
TERNAZIONALE
SUPERIORE
TUDI AVANZATI
TRIESTE
Strada Costiera 11

INDEX

FE II EMISSION LINES IN AGNs

Chapter 1

The Fe II Spectrum.

I.1 Fe II in astronomy.

The lines of singly ionized iron are present in the spectra of a large variety of astronomical objects. They have been observed in solar chromosphere (see, e.g. Dere, Bartoe, and Brueckner, 1986) as well as in stars and in extragalactic objects. Fe II lines have been studied in Ae and Be stars (see, e.g. de Freitas Pacheco, Landaberry, and Lopes, 1986; Covino et al., 1986; Talavera, 1986; de Martino and Vittone, 1986), in cold giants and supergiants (Engvold, Jensen, and Kjeldseth Moe, 1983; Jordan and Judge, 1984; Brown, Ferraz, and Jordan, 1981; Steenbock, 1985), in T Tau (Merrill, 1927, Wackerling, 1970; Brown, Ferraz, and Jordan, 1984), in symbiotic stars (Muratorio, 1985; Marsi and Selvelli, 1987), in superluminous stars (Gallagher et al., 1981) and in cataclysmic variables (Friedjung, 1974; Penston, 1983; Johansson, 1983; Netzer and Wills, 1983; Viotti, 1976a; Friedjung and Malakpur, 1971). Among extragalactic objects these lines are known to be present in the spectra of Seyfert 1 galaxies and of a few quasars (Phillips, 1977; 1978a; 1978b; Collin-Souffrin et al., 1979; 1980; Joly, 1981; Netzer, 1980; Netzer and Wills, 1983).

This nearly ubiquity is due both to the high abundance of iron and to the fact that the temperature and the density in most astrophysical sources preferentially produce and excite Fe^+.

$^{56}_{26}Fe$ is produced, together with the other "metals" by the nucleosynthesis reactions that take place in stellar interiors but, because of its high stability, its fractional abundance is much higher than that of the other, less stable, elements (fig. 1).

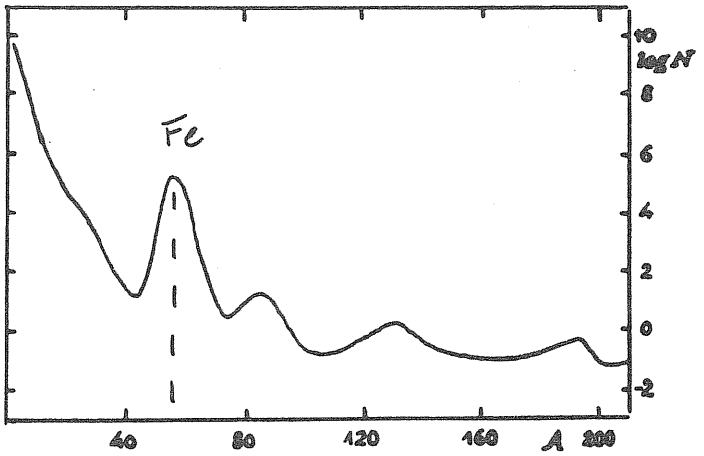

Fig. 1 : the abundance of the elements versus the atomic number.

The ionization of neutral iron is relatively easy, because the first ionization potential is quite low (χ_1 = 7.8 eV). Instead the second ionization is much more unlikely. The second ionization potential of Fe is of 16.1 eV, a value only a little higher than the ionization potential of hydrogen (13.6 eV). There is therefore a high probability that a photon having enough energy to ionize Fe^+, is absorbed by atoms of neutral hydrogen.

I.2 The Fe II atomic structure.

A very complex atomic structure is peculiar of Fe^+. Singly ionized iron has 25 electrons that, in the lowest energy case, are arranged in the configuration

$$(1s^2\ 2s^2\ 2p^6\ 3s^2\ 3p^6)\ 3d^6\ 4s$$

where the brackets include all the electrons that are located on complete orbits.

The values of the quantum numbers for the seven valence electrons and for the fundamental state of Fe^+ are given in Table I.

TABLE I

e^-	n	l	l_z	s
1	3	2	+2	+
2	3	2	+1	+
3	3	2	0	+
4	3	2	-1	+
5	3	2	-2	+
6	3	2	+2	-
7	4	0	0	+

In pure LS coupling the orbital angular momenta of the electrons interact together and give the total orbital angular momentum

$$\bar{L} = \sum_i \bar{l}_i$$

and a similar interaction of the individual spins gives the total spin of the system

$$\bar{S} = \sum_i \bar{s}_i$$

The set of states characterized by given values of L and S for a given configuration is called an atomic term.

The pure LS coupling is not exactly satisfied by Fe II because the $\bar{l}$ vector of each electron may interact with its own spin as well as with the orbital angular momenta of the other electrons and this condition is called intermediate coupling. "LS concept must then, in Fe II case, be considered as a level designation rather than a physical description of the state" (Johansson, 1984).

Some other parameters that we can evaluate are the multiplicity of the term, given by (2S+1) and its parity that is $(-1)^{\sum l_i}$.
The fundamental term of Fe II is then

$$a\,^6D$$

where the letter a stands for

$$3d^6\,(a\,^5D)\,4s$$

that is the configuration of the seven valence electrons together with the parent term. This is the term resulting from the six valence electrons of doubly ionized iron and it is very important to define better the state of the system.

We report here some cases in which the knowledge of the parent

term is fundamental to understand the FeII spectrum:

- Terms that are apparently equal can have different energies because they have different parent terms.

e.g. The terms $a\,^4D$ and $b\,^4D$ correspond to the same configuration, have the same total orbital angular momentum, the same parity and the same multiplicity, but different energies:

$$a\,^4D = 3d^6\,(a\,^5D)\,4s\;\;{}^4D \ldots\ldots\ldots E \sim 8000\ cm^{-1}$$

$$b\,^4D = 3d^6\,(a\,^3D)\,4s\;\;{}^4D \ldots\ldots\ldots E \sim 31000\ cm^{-1}$$

- The probability of a transition is much higher if the parent perm does not change.

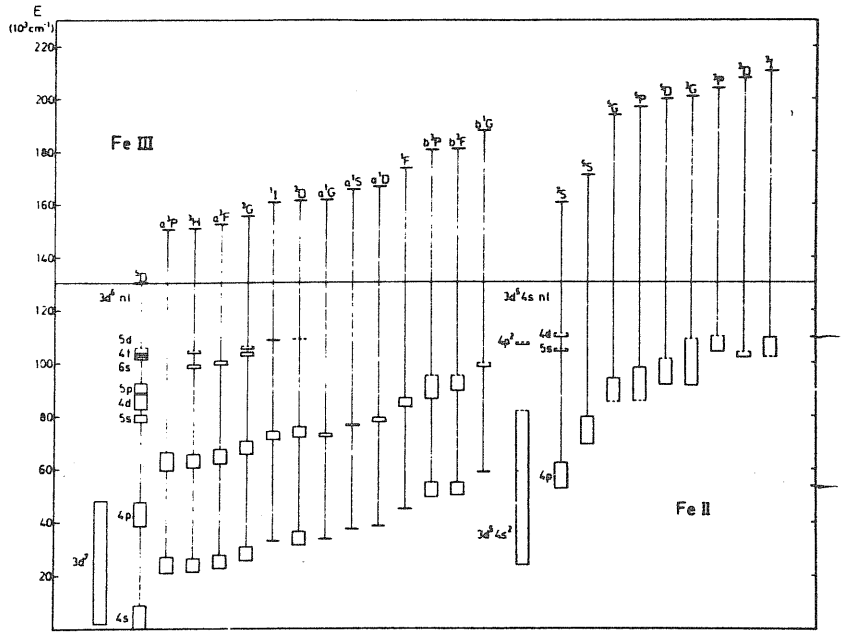

Fig. 2: the term scheme for Fe II: the transitions 4s - 4p and the 4p - 5s have similar energy differences.

e.g. The strongest lines of the Fe II spectrum (m = 1,2,3,...62,63,...78) correspond to 4s - 4p transitions of one

electron, without changing the state of the other six valence electrons. We remark also that these transitions, as well as the 4p - 5s transitions (corresponding to m = 380, 391, 399...) have energy differences that are very similar (fig. 2). This fact makes the 2000 - 3000 Å range extremely rich of FeII lines.

- The selection rules must not be violated for parent terms either. e.g. Some strong lines observed in the UV spectrum of many Fe II objects can be identified with the multiplets UV 190 and UV 191 (Engvold, Jensen and Kjeldseth Moe, 1983; Nussbaumer, Pettini and Storey, 1981). They correspond to the transitions

UV 191.....$a\,^6S$ - $x\,^6P^o$

$3d^5\,(^6S)\,4s^2\,(^1P)$ $3d^5\,(^6S)\,4s4p\,(^1P)$

UV 190.....$a\,^6S$ - $y\,^6P^o$

$3d^5\,(^6S)\,4s^2\,(^1S)$ $3d^5\,(^6S)\,4s4p\,(^3P)$

UV 190 has the character of an intersystem transition and this fact is responsible for its lower probability (Johansson, 1984). In this example the parent term is that of the five d electrons of Fe IV because the two 4s electrons form a complete orbit and the coupling between the 4s and 4p electrons is much stronger than their individual coupling to the $3d^5$ core.

If a certain amount of energy is given to the ion one or more electrons jump to a less bound orbit. In general a great number of higher energy configurations is possible, they are usually divided into two systems:

$$(1s^2\ 2s^2\ 2p^6\ 3s^2\ 3p^6)\ 3d^6\ nl$$

$$(1s^2\ 2s^2\ 2p^6\ 3s^2\ 3p^6)\ 3d^5\ 4s\ nl$$

The interactions between the seven valence electrons of Fe II give then origin to more than a hundred of terms (Moore, 1952).

Another interaction must now be taken into account: the one between the $\bar{L}$ and $\bar{S}$ vectors of each term. This interaction gives origin to a new quantum number, the total angular momentum of the system:

$$\bar{J} = \bar{L} + \bar{S}$$

The set of states of a term having the same value of J is called a level. In the atomic structure of Fe II there are thousands of levels and over a million of transitions among them (Kurucz, 1981). Although the LS selection rules will reduce this number, we point out that, since the Fe^+ ion does not strictly satisfies LS coupling, the violation of these rules is quite common.

The spectral range covered by these transitions is very broad: 10^3 - 10^6 Å. The peculiar energy distribution of the lower energy terms, however, makes the near UV range (2000 - 3300 Å) very rich of strong resonance lines (see fig. 2).

The high complexity of the Fe II atomic structure can be seen even more easily by comparing its Grotrian diagram with that of Ca II (fig. 3). In both cases the transitions 4s - 4p and the 3d - 4p are the most important, but while in Ca II they correspond to the multiplets m=1 and m=2, that is five lines in all, in the

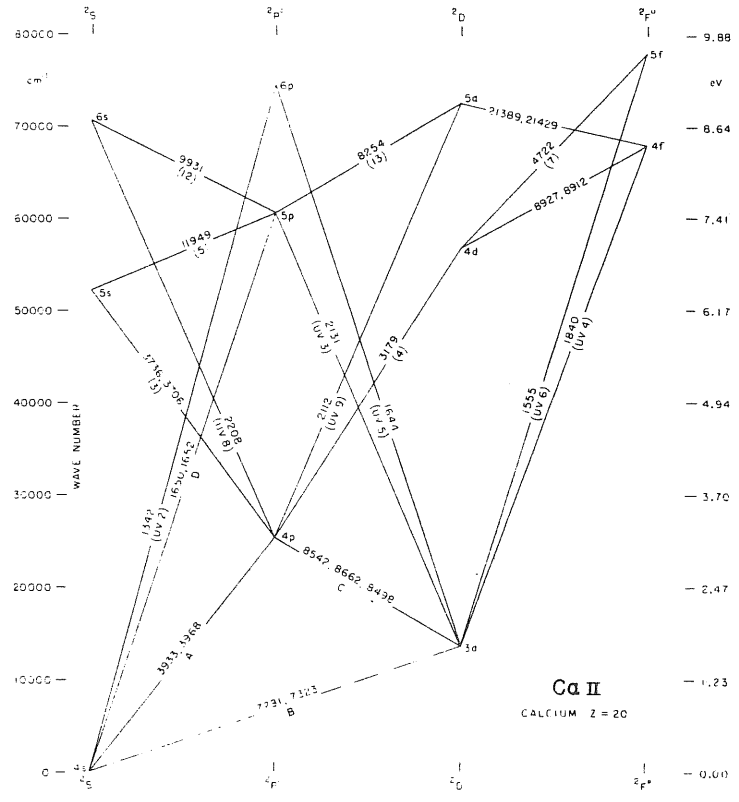

Fig. 3a : the Grotrian diagram for Ca II.

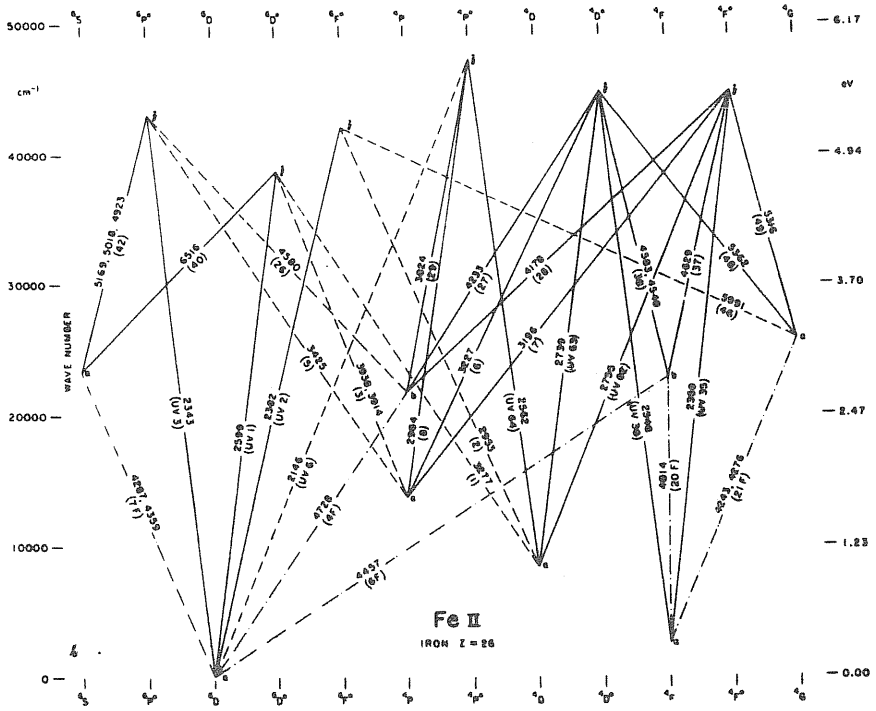

Fig. 3b : the Grotrian diagram for Fe II.

Fe II case they produce more than 1500 lines.

The Fe II Grotrian diagram of fig. 3b has been extremely simplified, being limited to the quartets and sextets of energy lower than about 5 eV (compare this value to the 16.1 eV that are needed for the second ionization of iron).

The various terms having the same total orbital angular momentum and spin are distinguished by a letter: a, b, c...for low-lying, even terms and z, x, y, w...for odd, upper terms.

Although the diagram is quite complex, some systematical behaviour can be found in the terms and in the transitions between them. There is a set of even, very low energy (E < 2 eV) terms, such as a^6D, a^4F, a^4D, a^4P that, although only a^6D corresponds exactly to E = 0, are usually called "ground terms".

At energies not much greater than 2 eV we can see some other even terms such as a^6S, b^4P, b^4F and a^4G that are connected to the ground terms only by forbidden transitions: they are the metastable terms.

Finally, at E~5 eV there are a number of odd terms (z^6P^o, z^6D^o, z^6F^o, z^4P^o, z^4D^o, z^4F^o) connected to the ground by permitted transitions. These terms are the upper terms of the most commonly studied optical and UV lines.

The energy difference between these tree sets is more or less constant, so, in a first approximation, the Fe II atomic structure can be simplified by a three-level representation (fig. 4). The resonance permitted lines (connecting ground and upper terms) fall usually in the near UV (2000 - 3300 Å) range, while the permitted transitions between upper and metastable terms give origin to

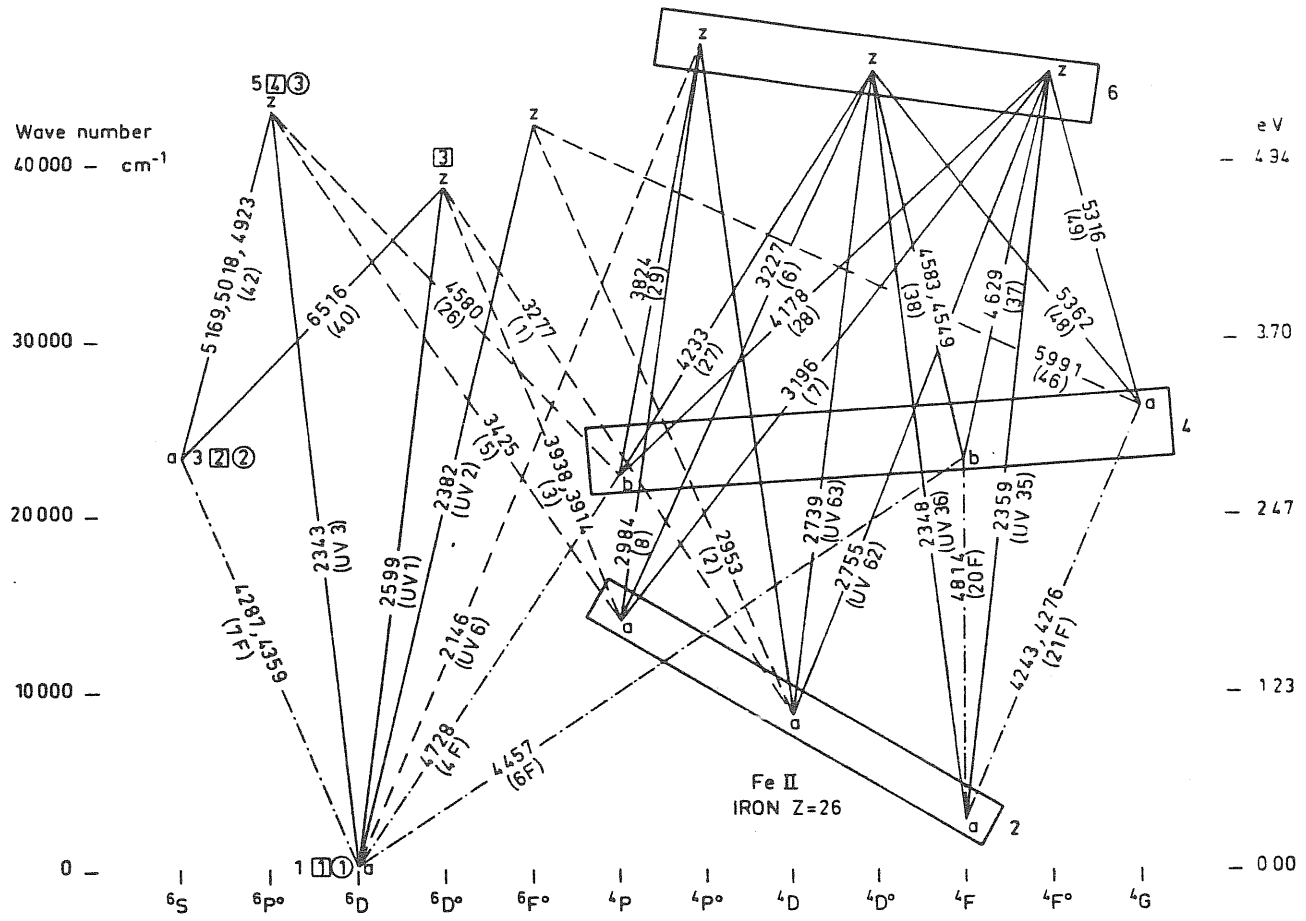

Fig. 4: a three- level representation of the FeII atom

optical lines. The forbidden transitions between the metastable and ground terms fall in the optical range also.

We point out, however, that although being a good zero-order approximation for the strongest resonance lines, this schematic picture loses a large part of its validity when the lines arise from higher energy terms or from terms belonging to the doublet system.

I.3 The present state of the knowledge of FeII.

The crowding of many strong lines into relatively narrow spectral ranges is the reason for the large number of Fe II blends that can not be resolved even in high resolution spectra. The measure of the individual line intensities in Fe II case is then generally a very hard task and becomes quite impossible if the resolution of the spectra is not very high. For this reason, the usually adopted method to study the observed spectrum is a comparison with a synthetic one. The construction of a synthetic spectrum for Fe II, however, is very complicated for a number of reasons.

The high complexity of the atom and the large number of lines that should be taken into account forces the authors to make several approximations. In the literature it is possible to find many works in which a more and more complex atomic structure for Fe II is assumed.

Viotti (1978b) assumes a simple, three-level structure for Fe II and a similar approximation is made by Collin-Souffrin et al. (1979). Netzer (1980) takes into account six terms and eight different transitions among them. In 1980, Collin-Souffrin et al. approximate the Fe II ion to a 9-level atom and one year later Joly (1981), in order to account for new UV data, extends the calculation to a 14-level atom. An even more complex atomic structure can be found in the work of Netzer and Wills (1983). They include all odd-parity levels of energies up to 9.1 eV and all even-parity levels having E < 7.5 eV, for a total of 70 terms and 1926 lines. Finally, Wills, Netzer and Wills (1985) extend previous

calculations to all levels up to 10.4 eV thus taking into account 3407 lines. This is, for the time being, the most complex atomic structure ever assumed for Fe II.

Another important problem is connected with the high energy terms, a great part of which is yet unknown. Term analisys of laboratory spectra of Fe II is going on (Johansson, 1986) and some important results, such as the discovery of new levels at 11 - 12 eV, can be found in Johansson (1984) and Johansson and Jordan (1984).

The next step toward the construction of a synthetic spectrum is the knowledge of the population mechanism.

The excitation mechanism is usually assumed as collisional (see, e.g. Collin-Souffrin et al., 1979; 1980; Viotti, 1976b) and/or radiative (Phillips, 1978b; Engvold et al., 1983; Jordan and Judge, 1984), but other, more exotic processes, can be responsible for the intensity discrepancies that are usually found between the observed and the theoretical spectra (Johansson, 1983). These processes include charge-exchange reactions between iron and hydrogen or helium as well as resonant photoexcitation by some strong emission line of another element (Ly α , Ly β , C IV λ 1550...).

Furelind (1984) suggests that in low density and low temperature cases the Balmer lines photons could ionize neutral iron and leave the resulting ions in an excited state.

All these processes can be inserted in a model only if the rate at which they take place is known. This means that a very large amount of atomic data, such as log gf's, collision strengths and

charge-exchange rates must be calculated. Although a lot of work has been done in this direction and is at present going on, the great dearth of atomic data, expecially of collision strengths and charge-exchange rates is remarked by many authors.
The most complete sample of semi-empirical log gf's can be found in the work of Kurucz (1981). He lists more than 20000 transitions between observed energy levels. The lines are characterized by log gf > -10 and 900 Å $< \lambda <$ 100,000 Å. Moity (1983) presents experimental log gf's for 494 Fe II lines falling in the 2500 - 5500 Å range and new measurements are in progress in the wavelength range 4000 - 8000 Å (Moity, 1986).

The collision strengths have been evaluated for some lines by Nussbaumer and Storey (1980). They give collision strengths for the lowest four terms of Fe$^+$ together with the relative forbidden transition probabilities and the transition probabilities of multiplets UV 1, UV 2 and UV3. In a following paper (Nussbaumer, Pettini and Storey, 1981) they extend their previous calculations and give the collision strengths for these transitions too and the electric dipole transition probabilities from the terms ^6P, ^6D, ^6F and ^8P of the configurations $3d^6 4p$, $3d^5 4s4p$ and $3d^6 5p$ to a ^6D. But, with the exception of these few data, the collision strengths are generally computed from log gf's values, according to a semiempirical method established by Seaton (1962)..

The knowledge of charge-exchange rates is even more approximate. Some values are given by Netzer (1980) and by Joly (1981), but they are only rougth extimations.

In addition to the problems mentioned up to now, the spectral

properties of a transition element like iron must be taken into account. The 4s and 3d electrons have nearly equal binding energies, so the low energy configurations

$$(1s^2\ 2s^2\ 2p^6\ 3s^2\ 3p^6)\ 3d^7$$

and

$$(1s^2\ 2s^2\ 2p^6\ 3s^2\ 3p^6)\ 3d^5\ 4s^2$$

can easily interact with the fundamental one. "This interaction complicates the calculation of the atomic structure and reduces the reability of calculated oscillator strengths" (Johansson, 1983).

Finally, since the Fe^+ ion does not strictly satisfies pure LS coupling, the forbidden and intercombination lines have relatively high transition probabilities. Such a fact becomes particularly troublesome if we consider that about half of Fe II miltiplets consists of intercombination lines (Moore, 1945).

Chapter II

The Active Galactic nuclei

II.1 Introduction.

The earliest observations of active galaxies date back to the first half of this century, when Fath in 1908 and Hubble (1926) remarked the presence of a few nebular lines in the spectra of NGC 1068, 4051 and 4151. In 1943 Seyfert included these objects in his list of "peculiar" galaxies. All Seyfert galaxies showed high ionization emission line spectra with wider lines than in normal galaxies and a very luminous nucleus.

Twenty years later several nebular emission lines were identified in the star-like, thirteenth magnitude object 3C 273 (Schmidt, 1963) and its redshift ($z = 0.158$) was measured. An even higher redshift ($z = 0.367$) was measured in the same year in 3C 48 (Greenstein and Matthews, 1963). If the redshift had cosmological origin then, quasi-stellar radio-sources appeared to be the most distant and most luminous objects in the universe. The identification of quasars with galactic nuclei was supported, years later, by the discovery, in some objects, of a faint nebulosity around them, having approximately the same angular size and apparent luminosity of a spiral galaxy at the distance indicated by the redshift (Osterbrock,1987).

Seyfert galaxies and quasars are now collected under the unique definition of active galactic nuclei, where the word "active" means that there is some evidence that the radiated energy can not be produced in the usual nucleosynthesis reactions in stellar

interiors. In Seyfert galaxies and quasars the activity is indicated by the presence of a very intense, point-like continuum source and many strong and broad emission lines, but there are many other classes of AGNs, with different defining characteristics. Among primary classifying criteria there are: polarization and variability of the emitted radiation, luminosity of the nucleus relative to the underlying galaxy, radio to optical luminosity, width and strength of the emission lines, morfology of the radio source, and so on. The various classes of AGNs, together with their principal properties, are collected in table II (O'Dell, 1986).

TABLE II

Summary of Properties of AGNs

Class of AGN	Radio	Optical Lines	Optical Pol.	Optical Var.	X-ray	Host Galaxy
Blazars:						
OVV and HPQ	s c	s 1	s	m-s	s	E?
BL Lac objects	s c	w	s	m-s	s	E
Optically quiet	s c	w	s	m-s	s	E
Radio Galaxies:						
Broad-line (BLRG)	s(c)	s 1	w	w-m	s	E, N
Narrow-line (NLRG)	m-s	s 2	w	w	w	E
Stellar-spectrum	m	w	w	w	m	E
Seyfert galaxies:						
Seyfert 1-1.5	w	s 1	w	w-m	s	S
Seyfert 1.8, 1.9	w	s 2+1	w	w	m	S
Seyfert 2	w-m	m-s 2	w	w	w	S
LINER	w	w-m 2	w	w	w	S
Quasars (normal):						
Radio-loud (QSS)	s(c)	s 1	w	m	s	E?
Radio-quiet (QSO)	w	s 1	w	m	s	S?
Narrow-line [rare]	w	s 2	w	w-m?	m-s	S?

Explanation of symbols used in table:
s = strong — 1 = broad lines (2,000-20,000 km/s)
m = moderate — 2 = intermediate width (500-2,000 km/s)
w = weak — 3 = narrow lines (≤ 300 km/s)
c = compact radio source prominent

II.2 Observational aspects.

As already mentioned, AGNs are very luminous objects. The optical luminosities range from about $10^{9} L_{\odot}$, that is the thereshold above which a galactic nucleus can be classified as "active" upward to about $10^{15} L_{\odot}$ during the major outbursts of the high redshift AGNs.

Generally the luminosity in the optical band is much higher than that in the other spectral ranges. Typical values for the radio and X-ray emissions are

$$10^{-4} < L(\text{radio})/L(\text{opt.}) < 10^{-1}$$

and

$$10^{-3} < L(\text{X-ray})/L(\text{opt.}) < 1$$

(O'Dell, 1986 and ref. therein).

The emitted radiation can be interpolated by a power-law continuum of the form

$$F_{\nu} \propto \nu^{-\alpha}$$

but it is only a rough approximation, caused by our yet still poor knowledge of the continuum emission mechanism. We make an equivalent approximation when we assume the Plank's law to represent the continuum of a star.

A unique power-law, however, hardly fits the entire spectral distribution, from radio to x-ray. The observed continuum is better represented as the resultant of two or more components,. In particular the optical continuum is well fitted by a power-law with

spectral index

$$\alpha \sim 1 - 1.5$$

extending down to infrared, while UV continuum has a flatter distribution. Usually the continuum flux in the approximate wavelength range 3000 - 4000 Å is not included in the determination of α, because in this spectral region many objects show an excess emission (Phillips, 1978a and ref. therein). In fig. 5 this broad hump is visible in the optical spectrum of 3C 120.

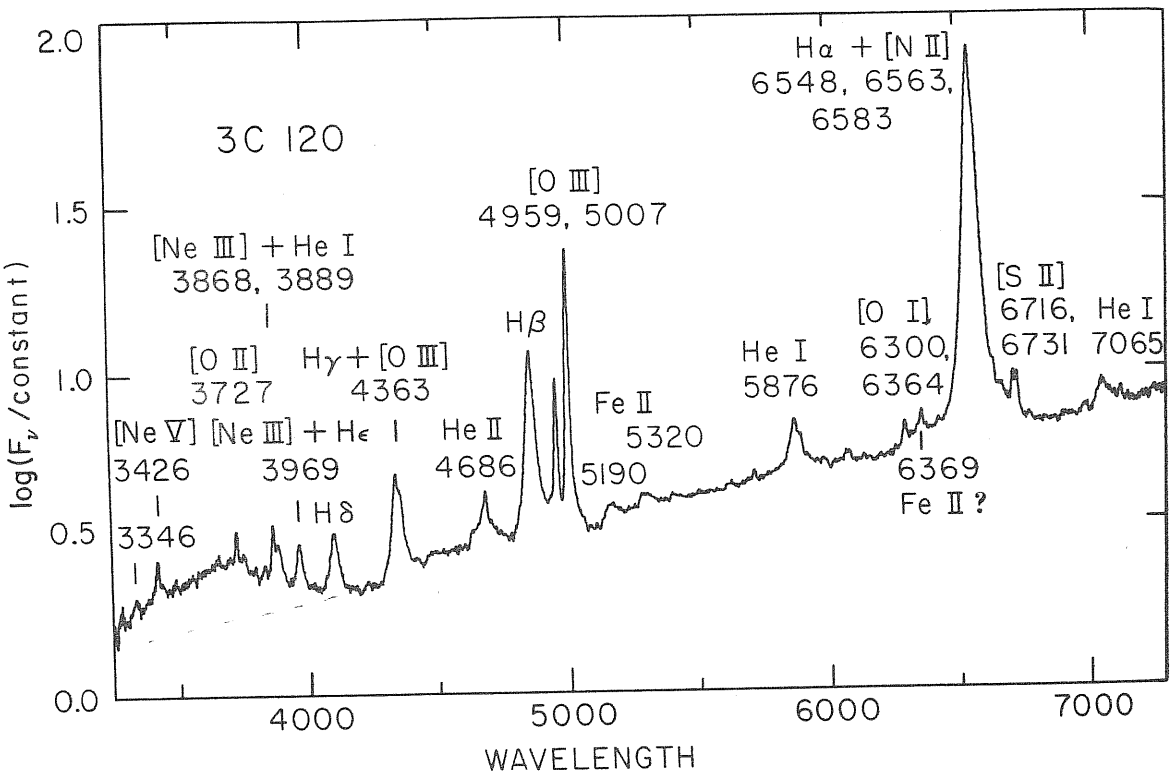

Fig. 5 : The optical spectrum of 3C 120: a broad hump is superimposed on the power-law continuum in the range $\lambda\lambda$ 3000 - 4000 Å.

Among X-ray sources two different shapes can be identified. In the first case a steep ($\alpha \sim 2 - 3$) soft-X (E < 1 KeV) component is superimposed on a flatter one extending to hard-X (fig. 6) while in the other a moderately steep ($\alpha \sim 1$) continuum extends from 0.2 KeV to 10 KeV (Elvis, 1986 and ref. therein).

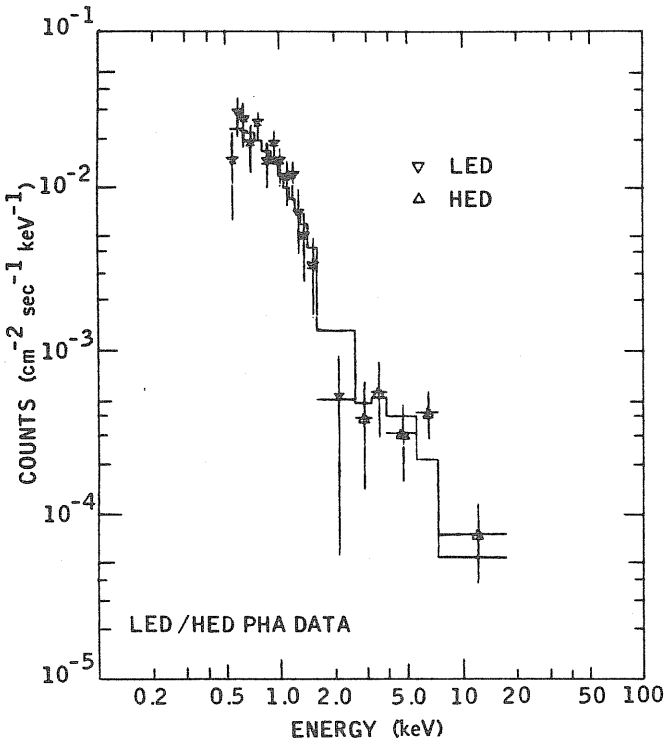

Fig. 6 : The X-ray spectrum of E 1821 + 643: a steep excess is visible in the soft-X range.

Above this featureless continuum the line spectrum is superimposed. In low luminosity AGNs some lines can appear in absorption. They are due either to the integrated spectrum of the host galaxy or to dust extinction (Stein and Soifer, 1983). With the exception of these few cases, however, the line spectrum of the

AGNs is in emission. The emission lines are usually very strong, broad, and cover a very wide ionization range. The observed species can go from neutral elements like O I to highly ionized ones. Fe VII or Ne V (IP $\sim$ 100 eV) forbidden lines are usually present and sometimes also [Fe X] λ 6374 or [Fe XI] λ 7892 (IP $\sim$ 250 eV) are visible (Osterbrock, 1984 and ref. therein). Seyfert 2 galaxies show, on the average, lower ionization lines and even less ionized species can be found in LINERs. Low-ionization-nuclear-emission-region objects, which are also characterized by weaker lines and a lower luminosity, are probably the lowest-energy version of the AGNs.

The width of the lines can show large differences, depending both on the class of AGNs and on the kind of the transition. The forbidden lines with the exception of C III λ 1909 (Mac Alpine, 1986) are always "narrow" lines, with FWHM of the order of 300 - 500 Km/sec. We point out that the word "narrow" is referred to the other lines of the AGN, since also "narrow" lines are "broad" in comparison with the emission lines of normal galaxies. The permitted and intercombination lines of Seyfert 1 galaxies and quasars are instead referred to as "broad". Their FWHMs have typical values of the order of 2000 Km/sec but also more extreme values have been measured. For example in Mrk 279, 704, 876 and 926 the FWHMs are of the order of $6*10^3$ Km/sec, but they are about one order of magnitude lower in Mrk 42, Mrk 359 and Akn 564 (Osterbrock and Shuder, 1982).

In Seyfert 2 galaxies both permitted and forbidden lines have similar widths (about 500 Km/sec).

Finally a few Seyfert galaxies have been observed that show intermediate characteristics between Seyfert 1 and Seyfert 2. Some objects, like NGC 5548 or Mrk 704 show broad permitted lines with a narrow core, others have a broad Hα emission, but the other lines give origin to a typical Seyfert 2 spectrum, and a few show a broad Hβ emission too. They have been called respectively Seyfert 1.5, Seyfert 1.9 and Seyfert 1.8 (Osterbrock, 1981).

Among radiogalaxies it is possible to make a similar classification. BLRGs show broad permitted lines and narrow forbidden ones, while in NLRGs both permitted and forbidden lines are narrow. At present no narrow-line quasar has yet been observed. In fig. 7 the optical spectra of a Seyfert 1, a Seyfert 1.5, a Seyfert 2, a BLRG and a NLRG are given for comparison.

The space density of the various classes of AGNs ranges from about 10^{-4} to 10^{-9} objects/Mpc^{-3}. Radio-loud objects are relatively rare: only one galactic nucleus over about one hundred shows strong radio-emission.

In table III the space density of a few classes of galaxies is given (Osterbrock, 1982 and ref. therein):

TABLE III

Field Galaxies	$10^{(-1)}$ Mpc^{-3}
Luminous Spirals	$10^{(-2)}$
Seyfert Galaxies	$10^{(-4)}$
Radio Galaxies	$10^{(-6)}$
QSO	$10^{(-7)}$
QSS	$10^{(-9)}$

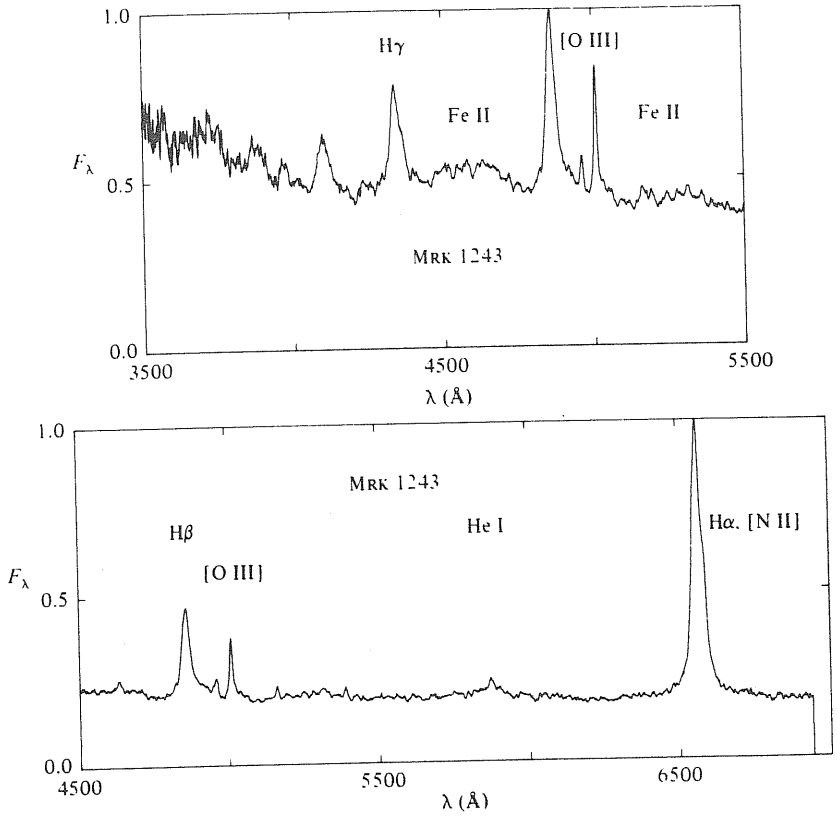

Fig. 7a : the spectrum of Mrk 1243, a typical Seyfert 1 galaxy

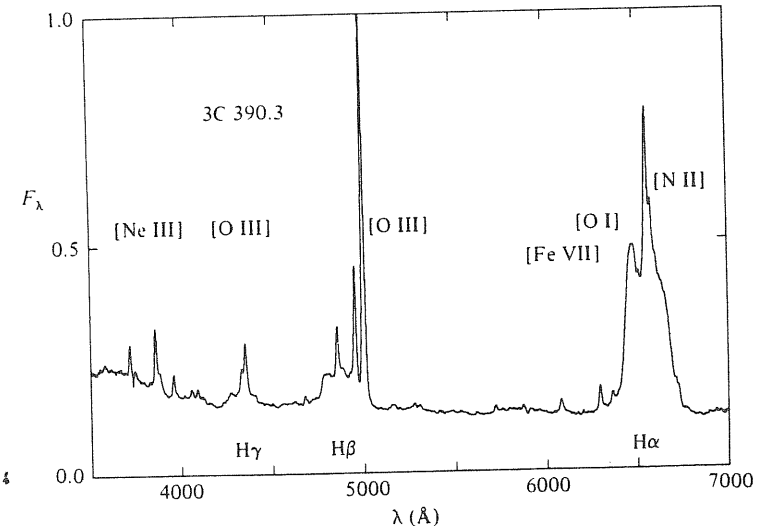

Fig. 7b : the spectrum of the BLRG 3C 390.3

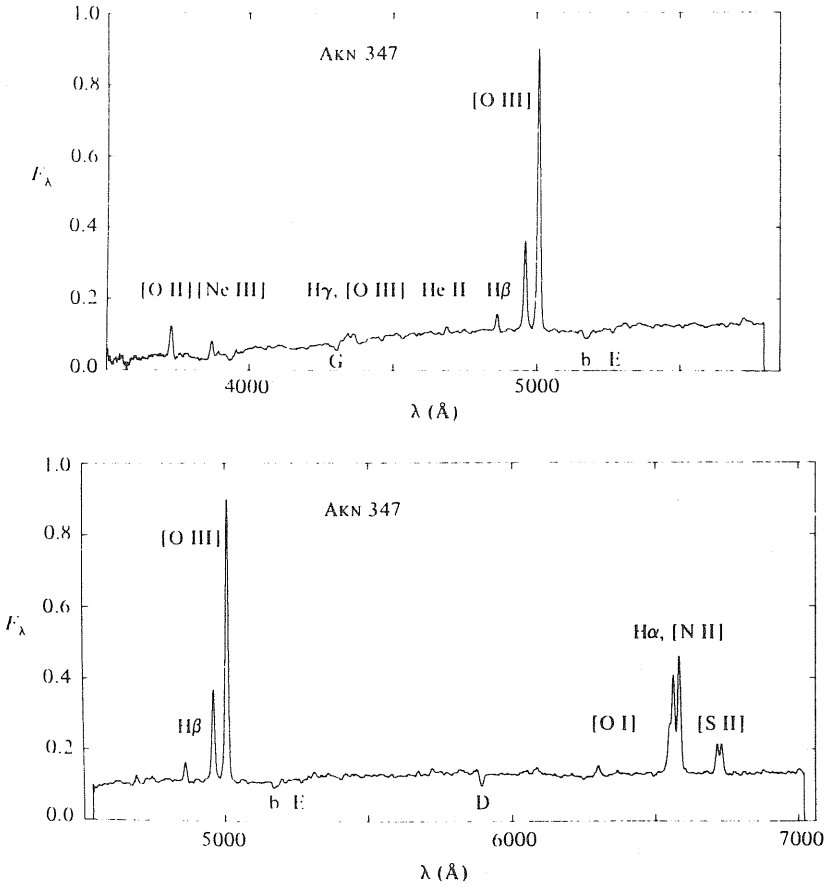

Fig. 7c : the spectrum of the Seyfert 2 galaxy AKN 347.

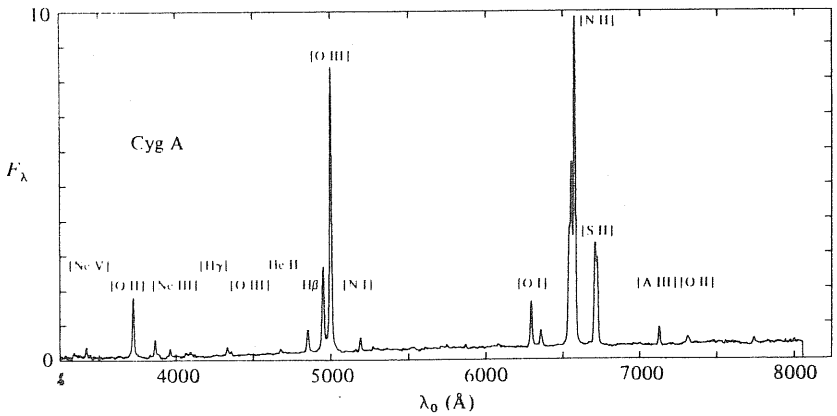

Fig. 7d : optical emissions of the NLRG 3C 405.

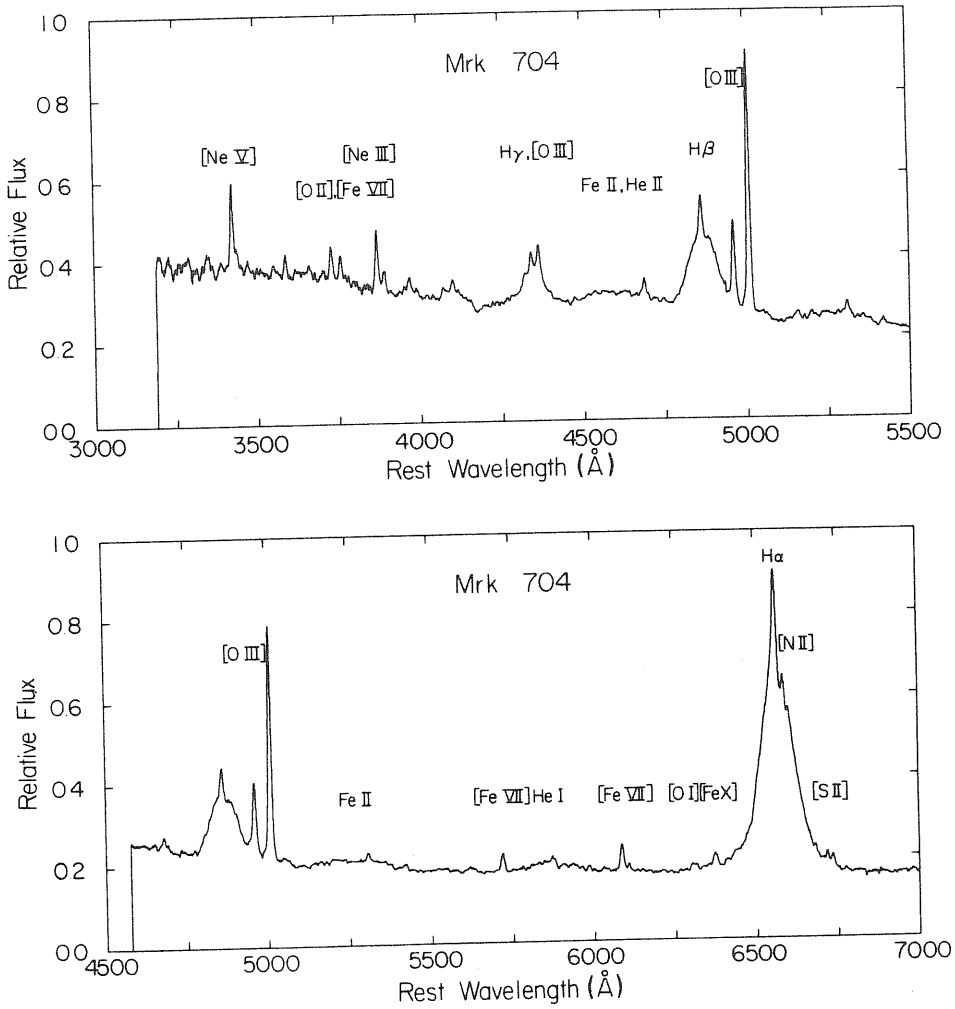

Fig 7e : the spectrum of Mrk 704, a typical Seyfert 1.5

Seyfert galaxies, however, although being very weak radio-emitters, are not radio-zero and their optical-radio frequency "colour index", defined as

$$P - RF = m_p + 2.5 \log S_{1415}\ (mJy) - 18.0$$

(Osterbrock, 1984) is of the order of some unities.

On the average Seyfert 2 galaxies are stronger radio-sources than Seyfert 1 and Seyfert 1.5 behave obviously in an intermediate

way (fig. 8).

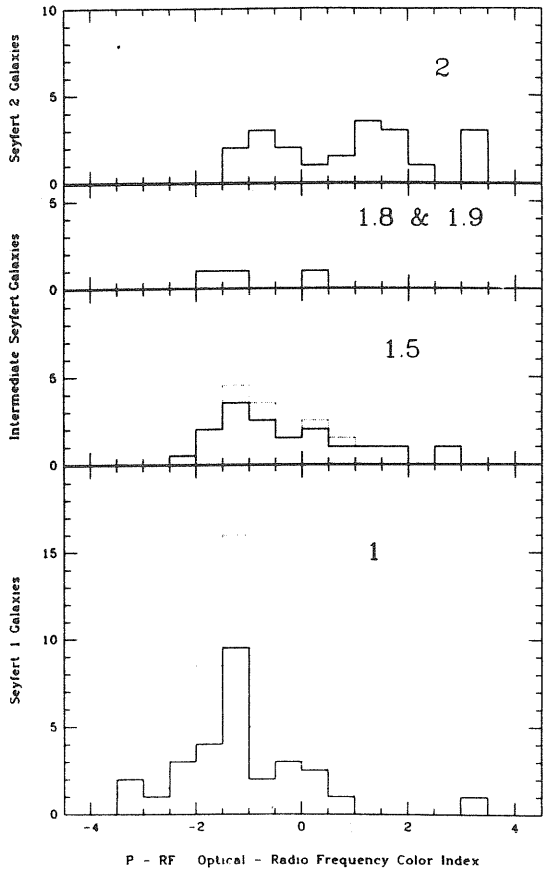

Fig. 8 : the Seyfert galaxy distribution according to their optical-radio frequency colour index.

Morfologically radio-galaxies are mostly extended double sources, with two radiolobes and a central compact component. Hine and Longair (1979), however, remark that the fractional luminosity of the central core to that of the extended components appears on the average to be higher in broad line objects than in narrow line ones.

Quasi stellar radio sources can be separated into three classes according to their radio structure (Miley and Miller, 1979).

About 50% of the observed QSS show a symmetric, double-lobed structure extending to more than 100 Kpc from the central object. They have steep spectra with spectral index

$$\alpha = - d(\ln S_\nu)/d(\ln \nu)$$

of the order of + 1.0.

The remaining quasars are instead core-dominated, but in many cases an extended, usually one-sided structure, smaller than 50 Kpc is visible. A typical example of this class is 3C 273. Finally, only about 10% of the quasars can be defined as "compact", since they have a radio structure smaller than 100 pc. The 16th magnitude, low-redshift quasar 3C 48 belongs to this class. Core-dominated sources are characterized by a flat spectrum, with

$$\alpha \sim 0$$

and in compact sources a cutoff at frequencies below 1 GHz can be found.

A peculiar feature, often observed in VLBI maps of the strongest, flat-spectrum radio-galaxies and quasars, is the presence of "superluminal" motions. Two components separating with an apparent transverse velocity of the order of 5 - 10 c are observed. Maps made at different epochs permit to follow this motion (fig. 9) and to exclude the possibility that the phenomenon is an illusion, something like the flashing "Christmas tree" lights (Condon, 1986).

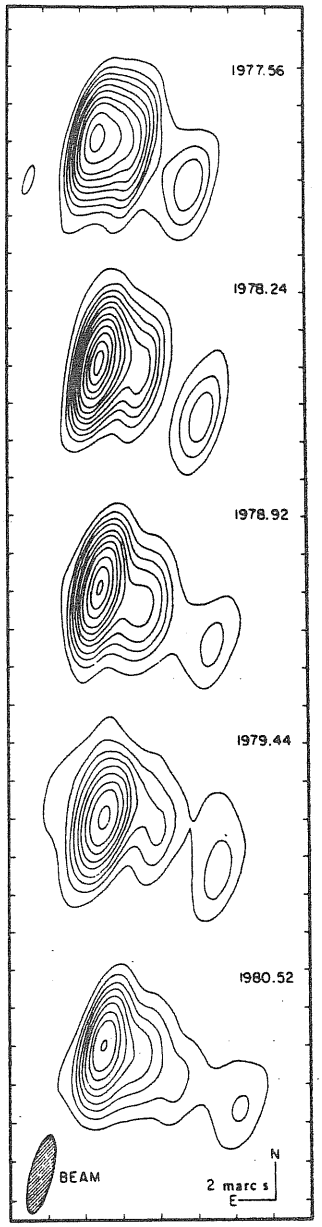

Fig. 9 : superluminal expansion in 3C 273

These relativistic jets are extremely well collimated, with apertures in the range 3^{o} - 15^{o}. Sometimes S-shaped configurations can be observed (Hunstead et al., 1984). A good example is the quasar 2300-189 shown in fig. 10.

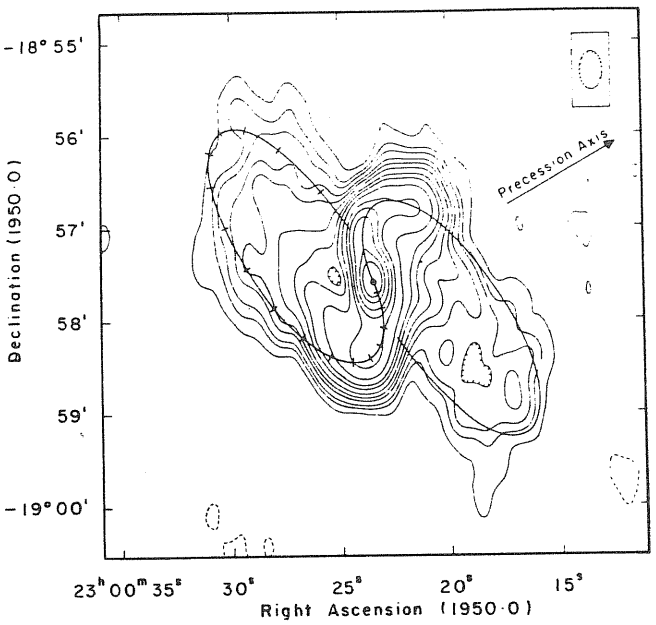

Fig. 10 : radio map of 2300-189.

In other cases the source is asymmetrical, with a nearly absent receding jet. Usually the jets are perpendicular to the plane of the galaxy but in some Seyfert galaxies some radio emission emerging from the nucleus along jets not aligned with the axis has been observed (Ulvestad, Wilson and Sramek, 1981; Booler, Pedlar and Davies, 1982).

I.3 The standard picture.

Unfortunately, the lack of informations, both on the central engine and on the way in which the emitted energy is reprocessed before leaving the AGN, makes it impossible to build up a complete model for the active nuclei. However, one can try to put together all these observational aspects, in order to draw a unique working picture, in which the various classes of AGNs are nothing else than different aspects of this unified scheme.

The high luminosity of the active nuclei puts some constrains on the mass of the central object. The total energy produced during the entire life of the most luminous AGNs can be strimates as much as

$$E \sim 10^{61} \text{ ergs}$$

(Condon, 1986). This corresponds to a central mass

$$M = E / \varepsilon c^2 = 10^6 / \varepsilon \; M_\odot$$

where ε is the conversion efficiency of mass to energy.

The central object must then be a cluster of stars or a supermassive object. The peculiar shape of the jets observed in the quasar 2300-189 and in some other objects is probably due to a precessing motion as can be seen by comparing the radio map of fig. 10 with the jet precession model (Hutching, 1983) for 2300-189 given in fig. 11. But since the precession model implies that the jet collimator is a rigid rotator, the hypothesis that the central object is a cluster of stars must be ruled out.

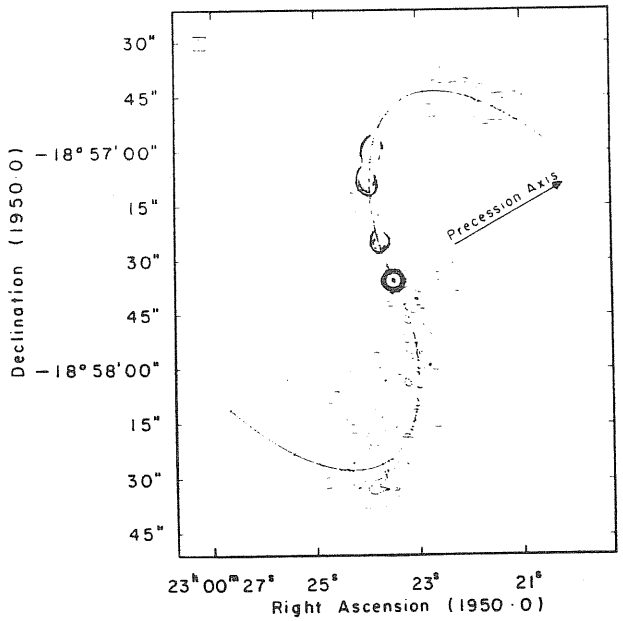

Fig. 11 : precession model for 2300-189.

Neither can it be a single, supermassive star. In fact a star should be pressure-supported along its rotational axis, so its luminosity must be of the order of the Eddington luminosity ($L_{Edd} = 10^{38} M/M_{\odot}$ erg/sec). For a supermassive star the maximum of the emitted radiation falls in the UV range and so one expects that AGNs are very luminous ultraviolet sources. As this is not true, one can conclude that there is something wrong in the single, supermassive star hypothesis.

The best candidates are then spinars (magnetically supported supermassive stars) and black holes, and this last possibility is supported also by other facts.

The idea that a black hole is the final result of the evolution of a galactic nucleus is widely accepted (Shields, 1986 and ref.

therein) and Serabyn and Lacy (1985) suggest the possibility that a compact dark mass of $3 * 10^{6}$ $M_{\odot}$ lies in the nucleus of our Galaxy. (The similarity of the structure of the central few parsecs of our Galaxy with a Seyfert 2 nucleus has been pointed out by Lo, 1986). In addition the small dimensions of the AGNs cause the need for a high mass to energy conversion in a small volume.

An usually accepted mechanism for extracting energy from a black hole is through accretion. The source of accretion, however, is not complitely known: the accreted matter can come from a tidal disruption of stars by the black hole (Hill, 1979) or from collisions of the quiescent galactic nucleus with intergalactic gas clouds (Gunn, 1979), in both cases it is assumed that the gas has sufficient angular momentum to form a disk (Shields, 1986).

The accretion rate can be estimated from the AGN luminosity. Disk accretion onto a black hole produces a luminosity

$$L = \varepsilon \dot{M} c^{2}$$

that assuming

$$\varepsilon \sim 0.1$$

becomes

$$L \sim 10^{46} \dot{M}/(1\ M_{\odot}\ yr^{-1})\ erg/sec$$

Since the Eddington luminosity for an object having mass M is

$$L_{Edd} \sim 10^{46} M/(10^{8} M_{\odot})\ erg/sec$$

the accretion rate for the most luminous AGNs must be of the order

of 1 $M_\odot$ yr^{-1}.

The tidal disruption of the stars however produces only a moderate accretion rate ($\dot{M} \sim 10^{-3}\ M_\odot\ yr^{-1}$) (Rees et al., 1982) so the most probable sources for the accreted matter must be the intergalactic gas clouds colliding with the AGN.

There is however another possibility, as suggested by Shields and Wheeler (1978). A much lower value for $\dot{M}$ is sufficient to explain the observed luminosity if the accretion is not constant. Matter can in fact be accumulated in the external regions of the disk for a long time and then be suddenly accreted onto the black hole. A similar mechanism, but on smaller scale, has been proposed by Smak (1984) to explain the outbursts of the dwarf novae. Both in this hypothesis and in the case of collisions with intergalactic clouds then, activity appears as a transitory phenomenon.

If the accretin disk is geometrically thin, it can be described by the "α - model" of Shakura and Sunyaev (1973). The high angular momentum of the infalling matter forces it to move on a Keplerian orbit around the black hole. The viscosity then redistributes the matter onto more and more bound orbits and in doing this some eneergy is locally dissipated. Radiative transfer then transports this heat to the surface.

The resulting disk appears to be divided into three zones: a "inner" zone, where radiation pressure and electron scattering dominate, and that is viscously and thermally unstable, a "middle' zone with gas pressure and electron scattering and an "outer", stable zone governed by gas pressure and Kramer opacity. The

dependence of the surface temperature on the radius can be evaluated in a steady state hypothesis: its asymptotic trend is

$$T \propto r^{-3/4}$$

If we assume that the disk is a collection of rings each one emitting like a black body at a given temperature, then, the slope of the resulting continuum can be calculated:

$$S \propto \nu^{1/3}$$

for

$$\nu_{out} < \nu < \nu_{max}$$

where

$$\nu_{out} = KT\,(R_{out})/h$$

$$\nu_{max} = 1*\,(M/M_{\odot})^{-1/4}\,(\dot{M}/\dot{M}_{cr})^{1/4}$$

with

$$\dot{M}_{cr} = L_{Edd}/\varepsilon c^{2}$$

For a supermassive ($M \sim 10^{8} M_{\odot}$) central object ν_{max} falls in the UV range and the evaluated trend fits well the flat UV continuum observed in many AGNs' spectra.

Another observational aspect is instead easily explained if the AGN accretion disk is geometrically thick. If $\dot{M} > \dot{M}_{cr}$ the radiation pressure thickens the inner part of the disk that appears torus-shaped. In the resulting axial funnels the radiation pressure

can accelerate the particles up to relativistic velocities in the axial direction and produce and collimate the observed jets (Jaroszynki, Abramovicz and Paczynski, 1980). An inclination of the disk plane with respect to the plane of the host galaxy can explain the non-alignment of the jets with the axis of the galaxy observed in some Seyferts (Tohline and Osterbrock, 1982). In such a picture, superluminal motions could be explained if the radio source is viewed in a direction near the axis of the jets. In the same time the apparently small flux of the receding jet is the reason for the observed one-sided sources. Double, extended sources could instead correspond to the edge-on point of view.

Around the disk there is the so called broad line region (BLR), where the broad emission lines originate. At the present our knowledge of the BLR is far to be complete because its small size (R $<$ 1 light-year) makes it impossible to resolve it from the Earth and because there are not good spectral diagnostics for the broad lines. However, many indications can be collected about its properties.

The width of the lines could be the result of the very high velocities at which the gas moves. In addition we can easily explain the wide range of FWHMs that we observe in Seyfert 1 galaxies if we assume a rotational motion in a cylindrical symmetry (Osterbrock, 1984). The relatively narrow lines observed in Mrk 359 and Akn 564 could infact indicate that the BLR is viewed "pole-on". Another possibility is the presence of a wind flowing out along the axis of the configuration.

The absence of broad forbidden lines, with the exception of

[C III] λ 1909, suggests that the electron density must be, on the average, in the range

$$10^{7} \leqslant N_{e} \leqslant 10^{10} \ cm^{-3}$$

but an inhomogeneous structure, with some denser regions together with more rarefied ones is probably present (Osterbrock, 1984; Phillips, 1978b).

The mass of the gas present in the BLR is then easily calculated

$$M \sim 10 - 10^{3} \ M_{\odot}$$

Only a rougth extimation of the temperature is instead possible, because of the lack of spectral diagnostics

$$T \sim 10^{4} \ K$$

The BLR is surrounded by a more rarefied zone, the narrow line region (NLR), into which it probably goes over continuously in density, velocity-field and inclination. This internal region is much more extended (100 - 1000 pc from the center) and highly inhomogeneous (MacAlpine, 1986). In the NLR clouds about $10^{4} - 10^{6} \ M_{\odot}$ of gas are present and move at velocities of hundreds of Km/sec. The electron density, the temperature and the chemical composition can be evaluated from forbidden line ratios. Typical values are

$$N_e \sim 10^{3} - 10^{6}\ cm^{-3}$$

$$T_e \sim 1 - 2 * 10^{4}\ K$$

and solar abundances.

Although the ionization mechanism for the BLR is not yet completely understood, there is little doubt in the NLR case. The similarity of its spectrum with that of the planetary nebulae and the difficulty to produce by collisions the observed high ionization species, strongly suggests that photoionization is the working mechanism. The photons emitted by the central accretion disk must then pass through the BLR. Since in a cylindrical configuration the BLR optical depth is lower along the rays near its axis than near its equator, the NLR ionization structure must reflect almost in part some axial symmetry too (fig.12).

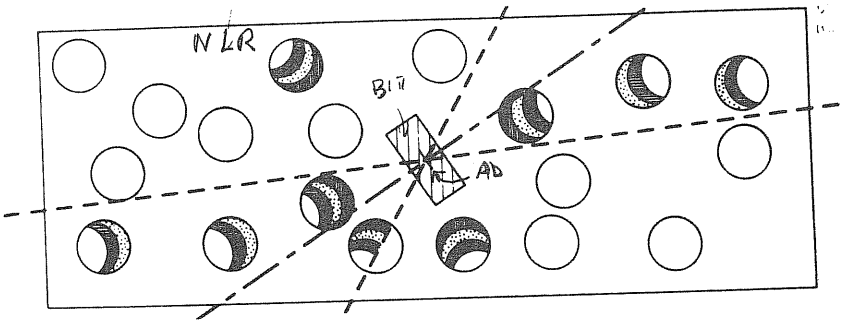

Fig. 12 : the standard picture for AGNs.

The NLR clouds are probably in pressure equilibrium with a surrounding hot, optically thin gas. Its estimated temperature is of the order of $1 - 2 * 10^{6}$ K so it could be the responsible for the excess usually observed in the soft-X range. Seyfert 1 galaxies

and quasars find a natural explanation in this picture, but it can fit rather well also other classes of AGNs.

In the case of Seyfert 2 galaxies, for example, the BLR could be hidden by a flat distribution of dust and become visible only through the light scattered by the electrons above and below the plane in which the dust is distributed (Antonucci and Miller, 1985).

On the other hand, the absence of lines in BL Lacs objects could be due to the absence of gas. IUE observations of Mrk 421 and 501 (Penston, 1982 and ref. therein) in fact, confirm the presence of a UV continuum extending below 1000 Å, of sufficient intensity to ionize hydrogen and produce detectable Lyα and Hβ.

Chapter III

The Fe II Spectrum in AGNs.

III.1 The Observations.

Fe II lines have been identified for the first time in the spectrum of an extragalactic object about twenty years ago. Wampler and Oke (1967) reported the presence of strong emission features at $\lambda\lambda$ 4450 - 4650 Å and $\lambda\lambda$ 5100 - 5400 Å in the optical spectrum of the bright, low-redshift quasar 3C 273 and identified them with blends of Fe II permitted lines. These lines are produced by transitions from odd quartets and sextets at about 5 eV ($z\,^4D^o$, $z\,^4F^o$, $z\,^6P^o$) to even metastable terms such as $a\,^4S$, $b\,^4F$, $a\,^4G$. These identifications were supported also by the presence, in Wampler and Oke's spectra, of some Fe II lines belonging to the optical multiplets m=1, m=6 and m=7. The Fe II forbidden lines on the contrary appeared to be very weak or absent. A few months later Sargent (1968) pointed out that the same emission lines reported above were present in the optical spectrum of the Seyfert galaxy I Zw 1 too, and subsequentely many Fe II emission lines were identified in nearly all of the known Seyfert 1 galaxies (see, e.g. Osterbrock, 1977). The blue spectra of two Seyfert 1 galaxies, I Zw 1 and Mrk 478 are given in fig. 13, with the identification of many Fe II multiplets.

The Fe II emissions are usually quite broad (FWHM $\sim$ 700 - 3000 km/sec). Phillips (1978a) points out that there must be a correlation between the width of the Fe II emission lines

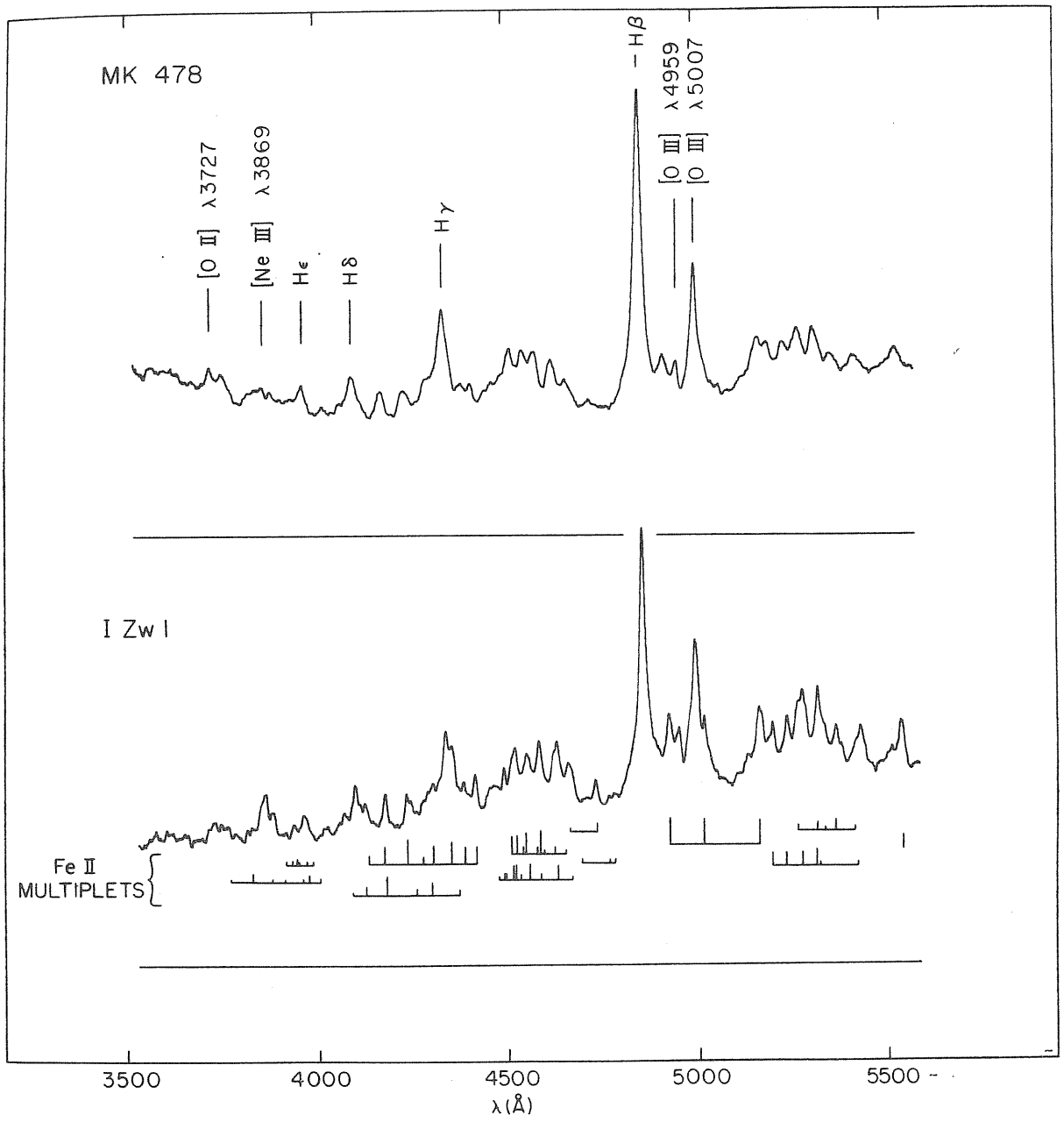

Fig. 13 : the optical spectra of the Seyfert galaxies I Zw 1 and Mrk 478, with the identifications of the strongest Fe II multiplets.

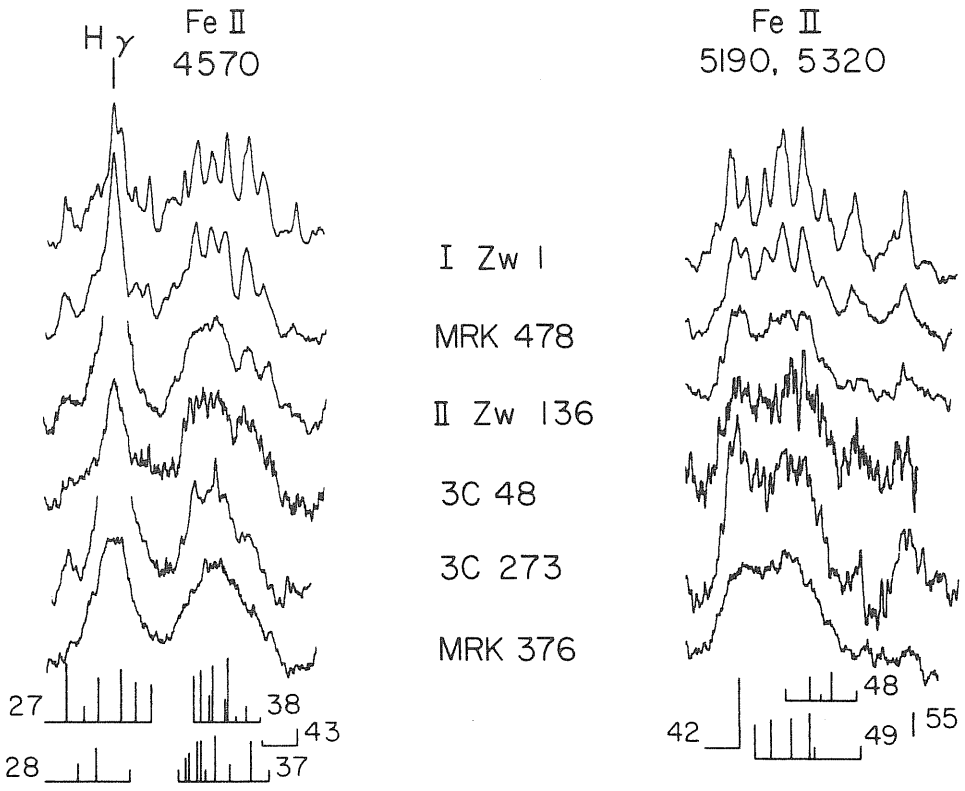

Fig. 14 : Fe II blends $\lambda\lambda$ 4570 and 5190, 5230 ordered according H γ width.

and that of the broad component of the hydrogen lines; as the width of H γ increases, the Fe II lines appear less and less resolved. The optical spectra of four Seyfert 1 galaxies and two quasars ordered according to Hγ width are given in fig. 14. Phillips (1977) remarks also that the Fe II spectrum of I Zw 1 is a good representative of a Seyfert 1 galaxy spectrum, since the only substantial difference is the width of the lines. In fig. 15 he compares the observed spectrum of Mrk 376 with that of I Zw 1, after a convolution with a Gaussian profile of the same width of

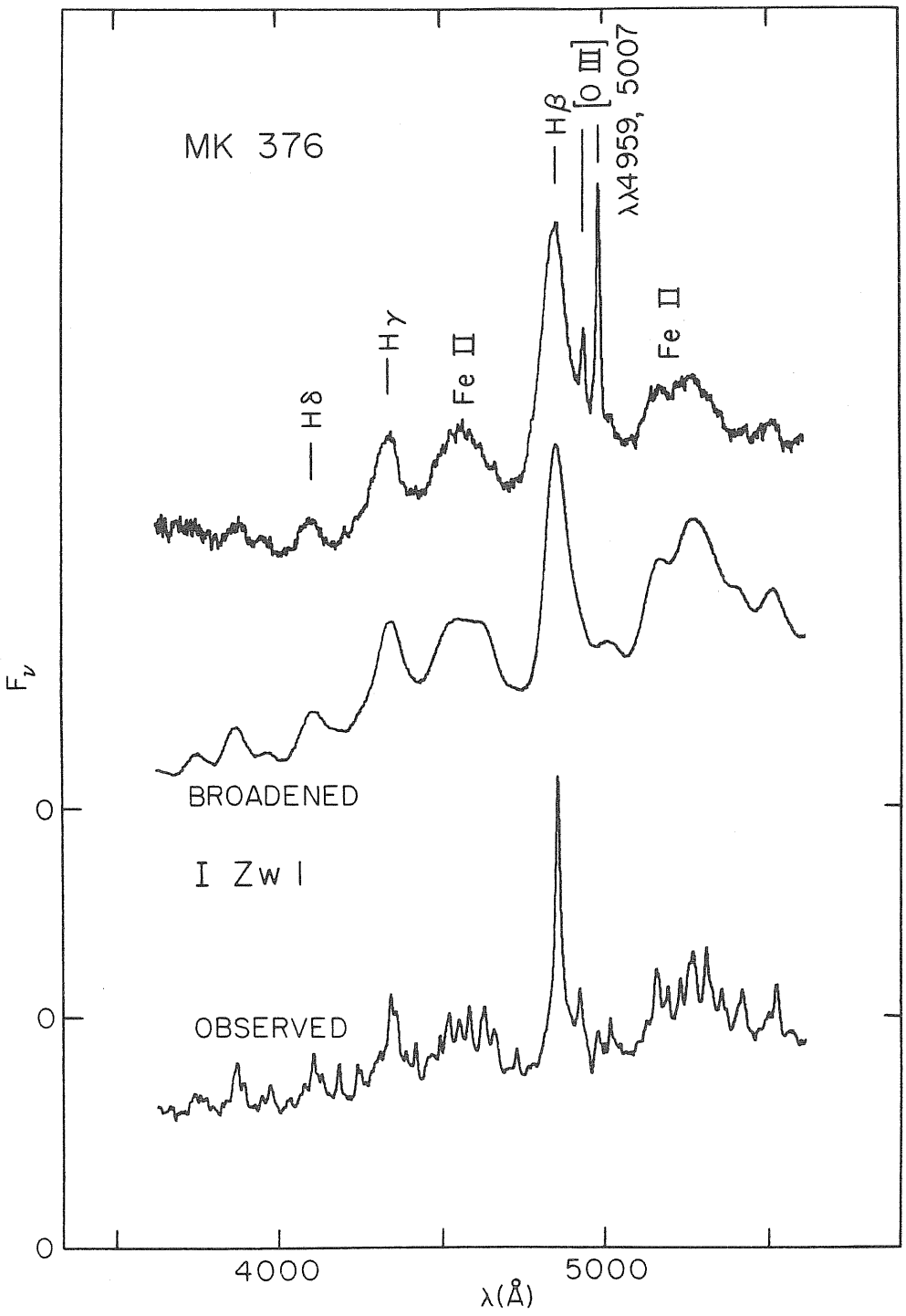

Fig. 15 : the observed spectrum of I Zw 1, after the convolution, can well represent the Mrk 376 emission features.

the $H\beta$ emission in Mrk 376: the agreement is quite good. All the observed lines correspond to permitted transitions, since the forbidden lines are usually very weak.

Boksemberg et al. (1977) tentatively identify with lines of [Fe II] some weak emission features around $\lambda\lambda$ 4230 - 4300 Å and $\lambda\lambda$ 4400 - 4430 Å observed in Mrk 231 and Oke and Lauer (1979) find that a few Fe II forbidden emissions are visible in the spectrum of I Zw 1. Their intensities are of the order of some units times 10^{-14} erg cm^{-2} sec^{-1}, that is, about 100 times weaker than $H\beta$. Since all these lines are blended with strong emission lines of other elements, however, both identifications are quite uncertain. In addition Joly (1981) finds that, with the exception of λ 5376 of m = 19F, they can all be identified with Fe II permitted lines.

In the optical spectra of the other classes of AGNs, even the broad permitted lines are hard to detect. The observed galactic nuclei include Seyfert 2 galaxies (Koski, 1978), NLRGs (Koski, 1978; Costero and Osterbrock, 1977) and BLRGs (Osterbrock, Koski and Phillips, 1975; 1976; Grandi and Osterbrock, 1978). Typical values for the strongest Fe II multiplets are

m = 37, 38:	I($\lambda\lambda$ 4515, 4520)	< 0.05 I($H\beta$)
m = 48, 49:	I(λ 5317)	< 0.05 I($H\beta$)
m = 48 :	I(λ 5363)	< 0.03 I($H\beta$)
m = 49 :	I(λ 5425)	< 0.03 I($H\beta$)

In fig. 16 the ratio Fe II/$H\beta$ is plotted versus $H\alpha$ /$H\beta$ for some BLRGs and Seyfert 1 galaxies: BLRGs show on the average much weaker

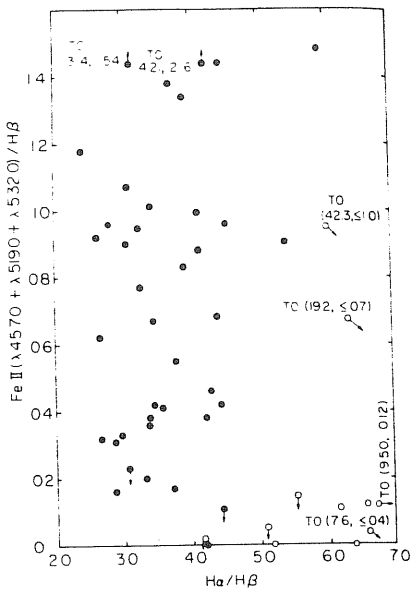

Fig. 16 : Fe II/ Hβ versus Hα /Hβ for Seyfert 1 galaxies (dots) and BLRG (circles).

Fe II emissions and a steeper Hα /Hβ ratio.

Fe II emissions are quite rare among quasars too, although 3C 273, the first extragalactic object showing Fe II lines was a QSS. Phillips (1977, 1978a) searched for Fe II optical lines in a sample of 20 QSOs at moderate redshift ($0.3 < z < 0.7$): only five of them showed detectable emissions, with

$$I(\lambda_{LAB}4750)/I(H\beta) > 0.1$$

It is actually rather surprising the fact that all these QSOs belong to the low-redshift wing of the sample, while no Fe II emissions have been observed in high redshift quasars. In a high-redshift object in fact the near UV range, where most of the strong Fe II resonance lines fall, should be accessible also from ground observations. Fe II UV lines instead appeared much weaker

than optical lines. For two of the quasars with detectable 4750, 3C 48 and PKS 1510-08 Phillips (1977) obtained the spectra down to a rest wavelength of about 2400 Å: "the observations revealed little evidence of either absorption or emission in <<resonance>> multiplets such as UV 1, UV 62, UV 63 and UV 64" (Phillips, 1978b). The spectra of these two quasars are shown in fig. 17.

Another peculiar aspect, present also in Seyfert 1 spectra, is the relative weakness of those multiplets, like m = 6 and m = 7 that fall in the near UV range. The upper terms of these multiplets $z\,^4D^o$ and $z\,^4F^o$, are the same of m = 37, 38, 48 and 49, and the branching ratio favours the near UV transitions for about 10 : 1 (cfr., e.g., Kurucz, 1981). The observed relative intensity is instead much weaker: the measured value in I Zw 1 is (Phillips, 1978a)

$$I(m = 6 + m = 7)/I(\lambda\,4570 + \lambda\lambda\,5190,5320) \sim 0.44$$

The UV range became accessible also for low redshift AGNs after the launch of the International Ultraviolet Explorer. Boksemberg et al. (1978) obtained low-dispersion spectra in the rest frame range $\lambda\lambda$1150 -3200 Å for several extragalactic objects, including two normal galaxies, a BL Lac object, the Seyfert galaxies NGC 4151 and NGC 1068 and the bright quasar 3C 273. No Fe II line, either in emission and in absorption, have been observed in 3C 273 and in NGC 1068 and a weak absorption feature, present in NGC 4151 is assumed by the authors to originate in an unusual absorbing region, "different from the BLR, that is typical of this object.

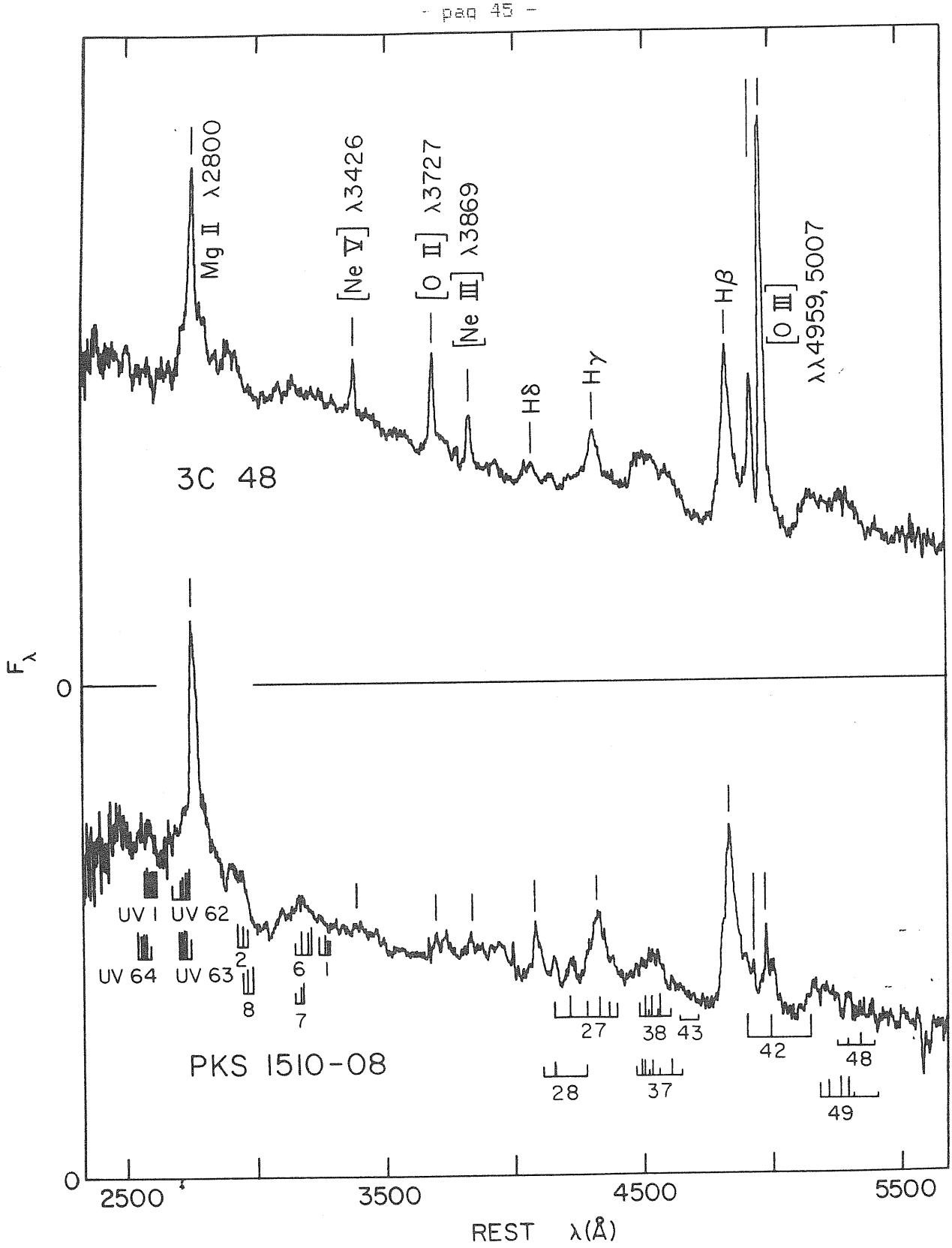

Fig. 17 : the near UV - optical spectra of the quasars 3C 48 and PKS 1510-08.

The weakness of the Fe II UV lines in 3C 273 is confirmed by Ulrich et al. (1980). They point out that this weakness applies both to resonance lines and to lines descending to even metastable terms (m = UV 35,UV 36, UV 62, UV 63...). In particular they find, for the multiplets m = 42 and UV 3, that share a common upper term ($z\,^6P^o$), a ratio

$$I(UV\ 3)/I(m = 42) \sim 0.4$$

The branching ratio, instead, favours the UV transition that should be about 100 times stronger than the optical one. They confirm, in addition, the presence of a similar deviation from the expected value for m = 6 and m = 7, as already noticed by Phillips (1978b).

A quite different result was obtained by Wills, Netzer, Uomoto and Wills (1980) from spectrophotometric observations of eleven intermediate redshift ($z \sim 1$) QSOs. They remark that some broad emission features at the rest wavelengths $\lambda\lambda$ 2300 - 2600 Å and $\lambda\lambda$ 2748, 2950 and 3200 Å are visible in the spectra of all the objects and they interpret these features as blends of Fe II resonance lines. In addition they point out that such features have already been observed, and tentatively identified with other elements, in many AGNs, but that these early identifications are not complitely convincing. They suggest that the $\lambda\lambda$ 2300 - 2600 Å feature could be produced by the multiplets UV 1, 2, 3, 33, 34, 35, 36 and 64, the one at λ 2748 by UV 62 and 63 and the emission at λ 2950 could be a blend of multiplets UV 60 and 61. Finally, the near UV multiplets m = 6 and m = 7 could be responsible for the broad feature observed at λ 3200 Å.

The relative intensities are referred to Mg II λ 2798, since direct comparisons with optical emissions are difficult:

$$I(\text{Fe II } \lambda\lambda\ 2300 - 2600)/I(\text{Mg II } \lambda\ 2798) \sim 1$$

$$I(\text{Fe II } \lambda\ 2748)/I(\text{Mg II } \lambda\ 2798) \sim 0.1$$

$$I(\text{Fe II } \lambda\ 2950)/I(\text{Mg II } \lambda\ 2798) \sim 0.1$$

The averaged value for the Mg II/Fe II opt. ratio in low redshift QSOs, then permits , in an indirect statistical way, an estimation of the UV/OPT. relative intensities:

$$I(\text{Fe II UV}) \sim 2 * I(\text{Fe II OPT.})$$

New relative intensities of Mg II with respect to Fe II m = 37, m = 38 have been measured by Bergeron and Kunth (1984) for a sample of 33 low and intermediate redshift QSOs. Some of their data are collected in fig. 18. A slight anticorrelation between the two lines is possibly present.

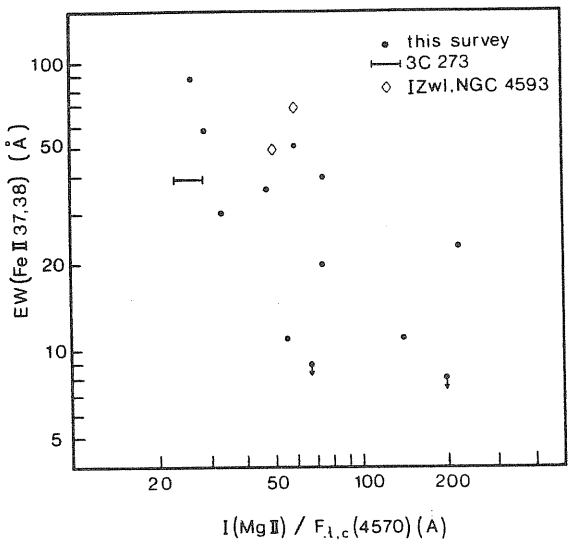

Fig. 18 : the equivalent width of Fe II m = 37, 38 versus the intensity of Mg II λ 2798.

In a subsequent paper, Wills, Netzer and Wills (1980) predict that some resonance emission lines originating from terms at about 8 eV must be present too. They observe these lines in the spectrum of PKS 2216-03 (fig. 19) and present literature references for previous observations of these features in other AGNs.

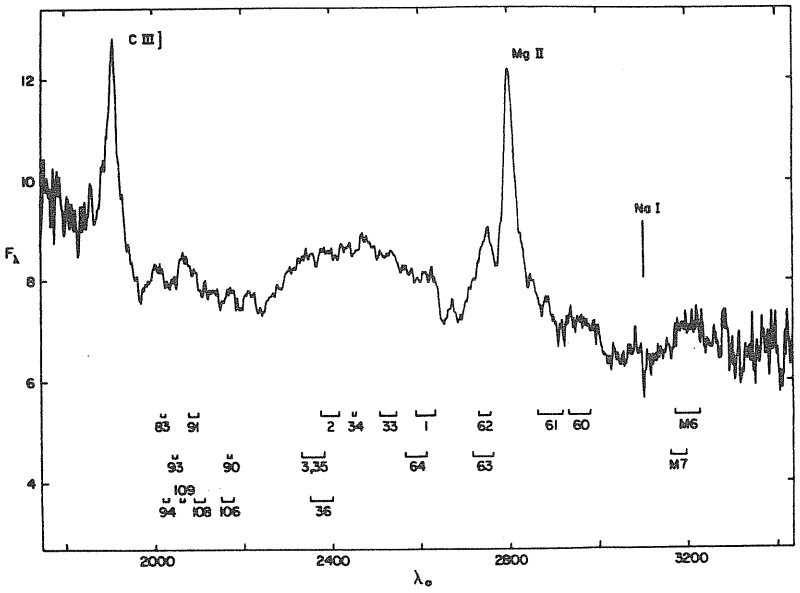

Fig. 19: Fe II multiplets arising from 8 eV terms in the spectrum of PKS 2216-03.

These lines are usually much weaker than those originating from 5 eV terms; some typical values are

$$I(\lambda\ 1860)/I(\lambda\lambda\ 2300 - 2600) \sim 0.15$$

$$I(\lambda\lambda\ 1610 - 1680)/I(\lambda\lambda\ 2300 - 2600) \sim 0.1$$

where the wavelengths are measured in the laboratory frame.

The possibility that relatively strong Fe II UV lines are a typical feature of intermediate and high redshift AGNs is ruled out by successive observations of low redshift objects.

Wills, Netzer and Wills (1985) observed seven low and intermediate redshift QSOs ($z < 0.7$) and found that Fe II is the largest contributor to the emission-line spectrum, providing more than 50% of the energy emitted by all the other lines together. The total intensity in the Fe II lines is one fourth of the intensity of Ly α and five times that of H β. An even higher ratio is found by Joly (1987) with Fe II tot./Ly α and Fe II tot./H β of the order of 2 and 12 respectively.

All the quasars in the sample of Wills, Netzer and Wills (1985) show strong Fe II UV lines, regardless of the strength of the optical lines, and the observed ratios are in the range

$$4 < I(\text{Fe II UV})/I(\text{Fe II OPT.}) < 12$$

They measured a quite high UV/OPT. ratio in the Seyfert galaxy Mrk 290 and in the BLRG 3C 390.3 too (Netzer, Wamsteker, Wills and Wills, 1985). The authors obtain simultaneous observations of these objects in the optical and UV range: in both cases the Fe II optical emissions are very weak while it is possible to observe strong UV features with relative intensity

$$I(\text{Fe II } \lambda\lambda\, 2000 - 3000)/I(\text{Fe II } \lambda\lambda\, 3500 - 6000) \sim 10$$

III.2 The excitation mechanisms.

The strongest Fe II emission lines observed in AGN spectra are produced by resonance transitions from odd parity levels at about 5 eV. In addition many weaker emissions whose upper terms lie at about 8 eV give a substantial contribution to the emitted energy in the wavelength range $\lambda\lambda$1600 - 2000 Å. The problem is then to find a mechanism that is able to populate these high levels and to account for the emitted energy.

The most likely excitation mechanisms are recombinations, collisional excitation, line and continuum fluorescence, but also more exotic processes like charge-exchange. reactions can be taken into account. Let's now consider more in detail the possible contribution of each mechanism to the emitted spectrum.

III.2 a Recombination.

It is very unlikely that the large amount of energy that is emitted in the Fe II lines is the result of recombination. To prove this one can evaluate the intensity of the Fe II optical lines in the recombination hypothesis and compare it with the intensity of Hβ . The choice of Hβ is due to the importance of this process in the excitation of neutral hydrogen.

In the most favourable hypothesis we can assume that the emission regions for Fe II and H coincide and that each recombination of Fe^{++} gives origin to an optical photon. If H is due only to recombinations then, the relative intensity is

$$\frac{I(\text{Fe II opt.})}{I(H\beta)} \lesssim \frac{N_e N_{Fe^{++}} \alpha_T(Fe^{++} \rightarrow Fe^{+})}{N_e N_{H^+} \alpha_{H\beta}}$$

where N_e, N_{H^+} and $N_{Fe^{++}}$ are the densities of the electrons and of the ions H^+ and Fe^{++} respectively.

$\alpha_{H\beta}$ is the effective recombination coefficient for $H\beta$ and is

$$\alpha_{H\beta} = 3.1 * 10^{-14} \text{ cm}^3 \text{ sec}^{-1}$$

$\alpha_T(Fe^{++} \rightarrow Fe^{+})$ is the temperature-dependent total recombination coefficient for Fe^{++} to Fe^{+}. An approximative estimation of this value for a temperature of 10^4 K is $7.3 * 10^{-13}$ cm^3 sec^{-1} (Phillips, 1978b, and ref. therein).

With the approximation

$$N_{Fe^{++}}/N_{H^+} \sim N_{Fe}/N_{H}$$

and assuming a solar abundance, a maximum limit for the relative intensity is

$$\frac{I(\text{Fe II opt.})}{I(H\beta)} \lesssim 7.6 * 10^{-4}$$

This value is more than three orders of magnitude lower than a typical ratio in a Fe II AGN and even the relative intensity of m = 37 alone in a Seyfert galaxy (see section III.1) shows a higher

value.

If some other mechanism contributes to Hβ emission or if the Fe II region is only a fraction of the H II zone, the discrepancy between the theoretical and the measured relative intensities becomes even larger.

Finally, only one recombination over one hundred produces an optical photon, since the branching ratio favours the UV transitions for about 100 : 1. In addition, if recombinations occur, also the higher energy levels such as the 8 eV ones should be strongly populated. The lack of emission lines from these terms in many objects provided to some authors (see, e.g. Phillips, 1978b) a further evidence against this excitation mechanism. Successive observations (Wills, netzer and Wills, 1980), however, led to the identifications of these lines in the UV spectrum of some quasars (see also fig. 19).

III.2 b Collisional excitation.

In the Fe II emission region a relatively high density

$$N_e \gtrsim 10^7 \ cm^{-3}$$

is suggested by the absence of [Fe II] lines (Osterbrock, 1984; Phillips, 1978a) and a temperature of 10^4 °K is typical (see, e.g. Phillips, 1978b).

At these physical conditions the electron collisions in the resonance-line transitions can significantly excite the Fe^+ ions and provide part of the emitted energy.

Although this process is assumed to be the principal responsible for the Fe II emissions by many authors (see, e.g. Collin-Souffrin et al., 1980; Joly, 1981) its estimated effectiveness is not very high. Phillips (1978b) evaluates the relative intensity of m = 42 with respect to Mg II λ 2798, line that is usually collisionally excited. In the hypothesis that Fe II and Mg II lines originate in the same zone (***) and that each collisional excitation in the $a^6D - z^6P^o$ transition leds to an optical m = 42 photon, the relative intensity is

$$\frac{I(\text{Fe II } m = 42)}{I(\text{Mg II } \lambda\ 2798)} < \frac{N_e N_{Fe^+}\ q(\lambda\ 2344)\ h\nu_{42}}{N_e N_{Mg^+}\ q(\lambda\ 2798)\ h\nu_{2798}}$$

where $q(\lambda\ 2344)$ and $q(\lambda\ 2798)$ are the collisional excitation rate coefficients in Fe^+ and Mg^+ resonance transitions respectively. They can be related to the collisional strengths by

$$q_{ij} = cost * \frac{\Omega_{ij}\ e^{-E_{ij}/KT}}{g_i \sqrt{T_e}}$$

(***) Bergeron and Kunth (1984) starting from the anticorrelation between Mg II and Fe II lines observed in their QSO spectra suggest that two different emission regions must exist for the two species.

If

$$\Omega\ (\lambda 2344) \sim 32$$

and

$$N_{Fe^+}/N_{Mg^+} \sim N_{Fe}/N_{Mg} \sim 0.79$$

the result is

$$I(\text{Fe II } m = 42)/I(\text{Mg } \lambda\ 2798) \lesssim 0.019$$

that is about one order of magnitude lower than the observed ratio. The discrepancy becomes even larger if some other mechanism contributes to the Mg II emission or if, as the branching ratio indicates, a substantial emission occurs also in m = UV 3. A good determination of the transition probabilities of m = 42 and UV 3 can be found e.g. in Nussbaumer, Pettini and Storey (1981).

The absence of the predicted Fe II UV emission lines in early AGN spectra (Phillips, 1977; 1978b; Ulrich et al., 1980) brought little support to the collisional excitation mechanism. Recent observations however (Wills, Netzer, Uomoto and Wills, 1980; Wills, Netzer and Wills, 1980, Netzer, Wamsteker, Wills and Wills, 1985; Wills, Netzer and Wills, 1985) have shown that UV lines are quite common, in good agreement with this process.

III.2 c Continuum Fluorescence.

In the continuum fluorescence process the high energy terms are populated by the absorption of ultraviolet continuum photons in the resonance line transitions. The UV resonance lines are then expected to appear in absorption and the observation of Fe II UV absorption lines in AGN spectra could be an immediate test of the occurrence of this mechanism (Phillips, 1977). The observed absence of these lines however, do not rule out the process because the resulting profiles are strongly dependent on the geometry of the emitting region. In particular the UV lines can appear in emission if the radiation comes from small discrete clouds and the covering factor is

$$\Omega / 4\pi < 0.01$$

(Collin-Souffrin et al., 1979) where Ω is the solid angle subtended by the clouds, as it is seen from the central object.

Phillips (1978b), however, evaluates that the energy emitted by the central source at the wavelengths of the Fe II resonance lines is sufficient to account for the observed emission in the optical lines only if a complete conversion of UV to optical photons occurs. The low covering factor that probably exists in Seyfert 1 galaxies and QSOs then, strongly reduces the efficiency of the process (Netzer, 1980). Netzer and Wills (1983) point out that although more than 1000 optically thick Fe II resonance lines are able to absorb in the UV range, the continuum fluorescence mechanism" accounts for only 10% of the energy emitted in the optical lines.

A strong argument against continuum fluorescence is the absence of Si II and Fe III emission lines in AGN spectra (Phillips, 1977). The resonance lines of these species fall at about 1000 Å (fig. 20) and an extrapolation of the power-law continuum down to this wavelength shows that there must be enough photons to produce detectable Si II and Fe III emission lines. In particular Phillips (1978b) evaluates that for a temperature of about 10000 °K a typical ratio is

$$I(Si\ II\ \lambda\ 5979)/I(Fe\ II\ \lambda\ 5169) = 0.46$$

If Si II and Fe II lines originate in a large transition (H^{o}, Fe^{+}) region, however, there is the possibility that the ionization of heavy elements such as C I, Mg I, Si I and Fe I significantly reduces the number of available continuum photons at $\lambda \sim 1000$ Å (Phillips, 1978b).

Instead, the absence of Fe III lines can be explained if we assume that some recombination mechanism such as charge-exchange with H^{o} (see section III.2 e) exists in the emission region (Collin-Souffrin et al., 1979).

Another objection comes from the observed absence of any correlation between the width and the intensity of the Fe II emission lines (Osterbrock, 1977; Phillips, 1978b; Bergeron and Kunth, 1984). Oke and Shield (1976) suggest that in a resonance fluorescence hypothesis this correlation must exist, since the objects that have broader resonance lines can absorb more UV continuum photons. Netzer (1980), however, remarks that the width of the absorption lines is not necessarily related to that of the

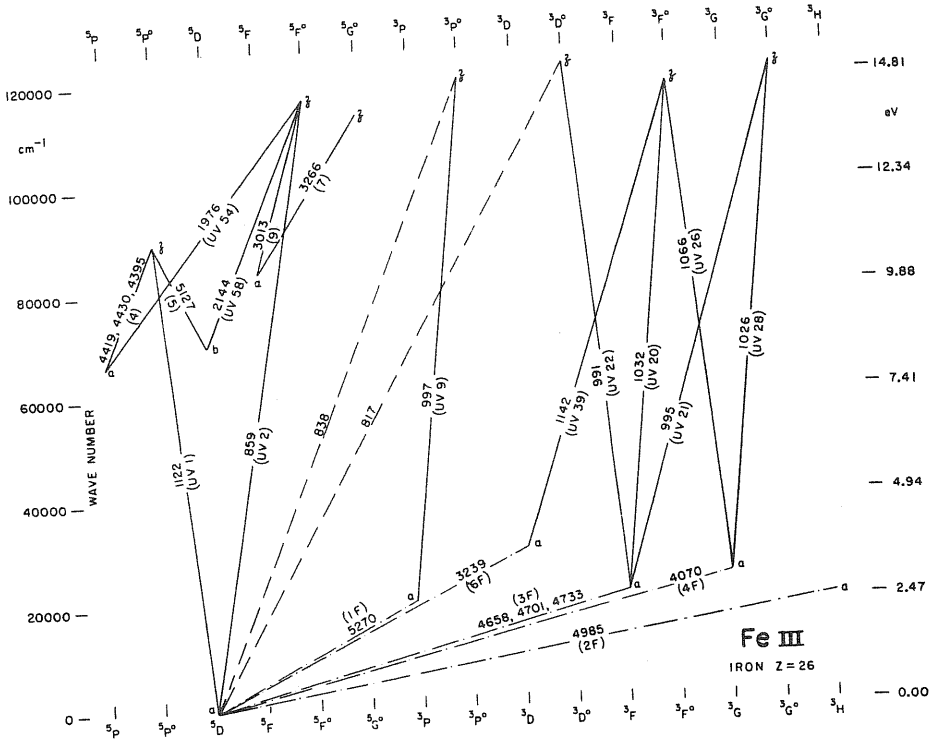

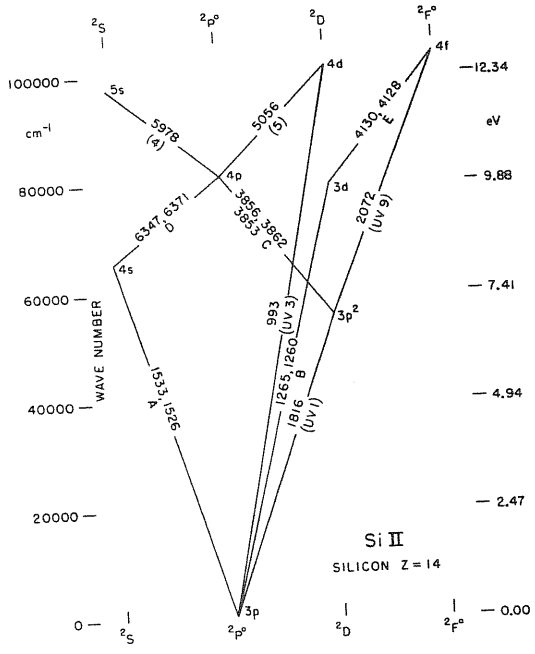

Fig. 20 : Fe III and Si II Grotrian diagrams.

emissions. If the BLR consists of a collection of clouds, the absorption profiles are broadened by the small internal motions inside each cloud (of the order of the thermal velocity), while the emissions reflect the high relative velocities (of the order of thousands of Km/sec) among them.

Phillips (1977) points out that the continuum fluorescence mechanism can explain the absence of Fe II lines in Seyfert 2 galaxies. These galactic nuclei have narrower lines and a less energetic continuum than Seyfert 1 galaxies or QSOs and so fewer UV photons can be absorbed. We remark, however, that the narrow emission lines originate in a different region, with a different mass distribution and dynamics, and do not necessarily reflect the presence of narrow absorption lines at the wavelengths of the resonance lines of Fe II.

III.2 d Line Fluorescence

The line fluorescence excitation mechanism is similar to continuum fluorescence. The fundamental difference is that the excitation energy is absorbed from an emission line instead of coming from the continuum. An accidental wavelength coincidence between the resonance line and an intense emission line of some other species is needed.

A well known example is the excitation of O III lines due to the absorption of He II Lyα photons at λ 303 Å that occurs in planetary nebulae, in AGNs and in other emission line objects.

The first suggestion that this mechanism could work for Fe II too is due to Gahn (1974). He remarked that many Fe II lines could

be excited by fluorescence with the Mg II doublet $\lambda\lambda$2798, 2802. Successively, many authors (Johansson, 1983; Penston et al., 1983; Brown, Ferraz and Jordan, 1981; Netzer and Wills, 1983) discussed the possibility that some emission lines observed in many astronomical objects but still unidentified could be Fe II lines produced by this mechanism. Accidental wavelength coincidences with Ly α, Ly β, C IV λ1548 and even among different Fe II lines have been considered and the efficiency of the mechanism has been found to depend on many factors.

The Fe II resonance line, or, more generally, the line corresponding to the upward transition, must have a large enough transition probability, in order to absorb a great number of the emission line photons. Since it is very unlikely that the wavelengths of these two lines coincide exactly, also near-coincidence cases are usually considered. The wavelength difference between the Fe II upward transition and the emission line of the other ion, however, must not exceed a few times the width of the lines. Beyond this limit in fact, the Fe II optical depth rapidly drops to zero. Finally, since the photons emitted by the other ion must be present in a great number in the Fe II region, an almost partial overlapping of the two emission zones strongly increases the efficiency of the process.

Netzer and Wills (1983) find that the contribution of the line fluorescence process to the Fe II spectrum, does not affect the total emitted energy, but can be responsible for the presence of some anomalously intense lines. The mechanism in fact works in a

selective way: only some upper levels appear to be overpopulated and only the downward transitions from these levels are strengthened. Observationally this means that only a few lines in a multiplet show an increased intensity. The authors, however, point out that for high enough electron density, the collisions can redistribute the line fluorescence contribution among the whole term and substantially complicate the picture. In addition they remark that an increasing fluorescence has the effect of producing weaker optical lines. In fact the optical transitions arise from relatively low levels (about 5 eV) whose population is reduced by the fluorescence process.

III.2 e Charge-exchange.

Another selective process that can affect the relative intensity of some lines, is the charge-exchange recombination mechanism.

In a charge-exchange reaction a neutral atom collides with an ion. During the collision one electron is exchanged leaving one of the species in an excited state (see, e.g. Johansson, 1984). The reaction can be schematized by

$$A^{+} + B \longrightarrow A + B^{+**} + \Delta E$$

where A and B are the two colliding atoms and ΔE is the energy defect:

$$\Delta E = IP(A) - IP(B) - EP(B^{+})$$

The dependence of the charge-exchange cross section on the energy

defect is given in fig. 21.

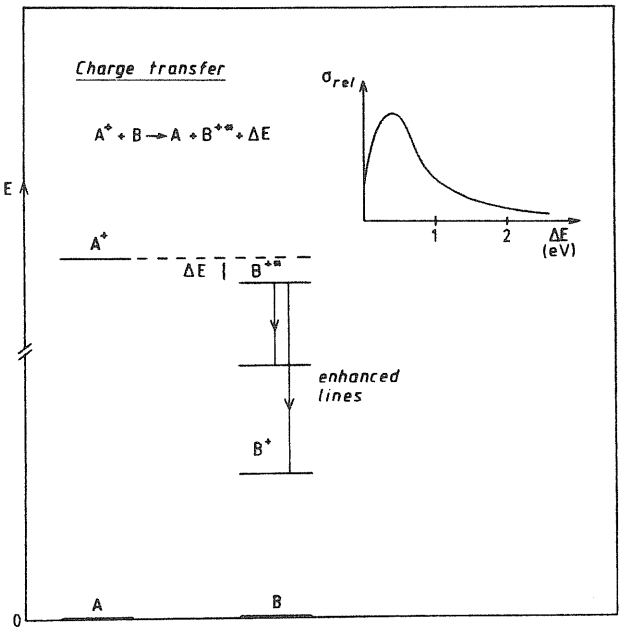

Fig. 21 : the relative energies and the cross section versus the energy defect in a charge-exchange process.

The possibility that charge-exchange reactions could excite the Fe^+ ions in an astrophysical plasma has been considered by Meyerott (1978). he finds that the most relevant processes are

$$Fe^+ + H \rightarrow Fe^{+**} (5.7\ eV) + H + \Delta E$$

that produces an overpopulation of the terms

z^6D^o , z^6P^o , z^4F^o , z^4D^o ;

$$Fe^{++} + H \rightarrow Fe^{+**} (2.5\ eV) + H^+ + \Delta E$$

that overpopulates the metastable terms and

$$Fe + He^{+} \longrightarrow Fe^{++} + He + e^{-} + \Delta E$$

The charge-exchange reactions with hydrogen can then produce two completely opposite observational results. A process of the first kind increases the upper term population of the most intense optical and UV transitions (see fig. 3b): m = 37, 38, 42, UV 2, UV 3, UV 35, UV 36... These lines appear then to be strengthened. The second reaction instead has the effect of increasing the opacity in the optical lines descending to the metastable terms, thus reducing the emission intensity of these lines. Reactions of the second kind can also explain the absence of Fe III lines in AGN spectra, lines that are predicted to exist if the excitation is due to continuum fluorescence.

Chapter IV

The Emission Models.

IV.1 Introduction.

The most usual approach for the interpretation of the various features in the analisys of the Fe II spectrum in AGNs is through the calculation of a synthetic model. The comparison between the observations and the theoretical expectations, permits the best estimate of the physical parameters of the emission region. Many attempts to compute the Fe II synthetic spectrum, under a variety of physical conditions can be found in the literature (see, e.g. Phillips, 1978b; Collin-Souffrin et al. 1980; Netzer and Wills, 1983). A scheme of the various models for the Fe II emission region, together with the assumptions about the ionization and the excitation mechanism is given in table IV. The presence of a dash means that the mechanism has not been included in the model. The word "no" means that the mechanism has been taken into account, but its estimated contribution to the emitted spectrum is negligible.

In this chapter we will describe some of these models: we will consider the assumed physical conditions and give some of their fundamental results.

TABLE IV

	ioniz. mech.		excit. mech.					geometry
ref.	(1)	(2)	(3)	(4)	(5)	(6)	(7)	
PS(1976)	-	yes	-	yes	-	-	yes	(a)
P(1978b)	yes	-	no	yes	yes	-	-	(b)
CS(1979)	yes	-	no	yes	yes	-	yes	(c)
CS(1980)	yes	yes	-	yes	yes	-	-	(d)
J(1981)	-	yes	-	yes	-	-	yes	(e)
N(1980)	yes	-	-	yes	yes	-	-	(f)
NW(1983)	yes	-	-	yes	yes	yes	no	(f)

(1) = photoionization
(2) = collis. ionizat.
(3) = recombination
(4) = collis. excitat.
(5) = continuum fluor.
(6) = line fluor.
(7) = charge-exchange

PS(1976) = Ptak and Stoner (1976)
P(1978b) = Phillips (1978b)
CS(1979) = Collin-Souffrin et al.(1979)
CS(1980) = Collin-Souffrin et al.(1980)
J(1981) = Joly (1981)
N(1980) = Netzer (1980)
NW(1983) = Netzer and Wills (1983)

(a) : radial flow
(b) : spherical distribution of homogeneous clouds
(c) : finite, homogeneous, plane parallels slab
(d) : extended accretion disk
(e) : finite, homogeneous slab
(f) : spherical distribution of non-homogeneous clouds

IV.2 The Suprathermal Particle Interaction.

One of the first attempts to explain the origin of the Fe II emission lines observed in Seyfert 1 galaxies and QSOs is due to Ptak and Stoner (1976). They assume that in the emission region there exist a radial flow of fast ($v \sim$ thousands of Km/sec) protons and other light ions. This stream of particles, that has a typical density of the order of 10^{4} cm^{-3} and a temperature of about 10000^{0}K moves through a partially ionized ambient gas (Ptak and Stoner, 1973). There are then two possible emission regions for the observed lines: the rapidly moving stream where the excitations are probably due to collisions and the ambient gas. Both the collisions and some charge-exchange reactions with the stream of protons are responsible for the gas excitation.

The broad Balmer lines are assumed to originate in the flow, and so do some other lines such as Ly α , C IV λ 1550, N V λ 1240, Si IV λ 1397, [Si III] λ 1888, and [C III] λ 1909 (Stoner, Ptak and Ellis, 1974).

The Fe II lines instead are emitted in a more dense ($N_e > 10^{7}$ cm^{-3}) region (Osterbrock, 1984; Phillips, 1978a) that has been identified with the ambient gas. In such an hypothesis, however, the Fe II lines should be substantially narrower than the Balmer lines (Ptak and Stoner, 1976). Phillips (1977) has found instead a strong correlation and a similar width between the Fe II lines and Hδ. On the basis of this observation he rules out the suprathermical particle model and assumes that both the Fe II and the H I emissions arise from the same region: a collection of discrete clouds or filaments in rapid relative motion.

IV.3 The Photoionization Models.

The usually assumption for the heating and ionizing of the emitting medium in Seyfert 1 galaxies and QSOs is the presence, in the BLR, of a continuum extending up to the hard UV range, that is emitted by the central source (Joly, 1981; Netzer, 1980).

In many cases the existence of such a continuum is sufficient to infer that resonance fluorescence must be the most important excitation mechanism (see, e.g. Collin-Souffrin et al., 1979 and ref. therein).

Phillips (1978b) evaluates the Fe II synthetic spectrum in the hypothesis of an optically thick and an optically thin emitting medium. Both resonance fluorescence and collisionasl excitation are separately considered. He takes into account 78 multiplets (about 475 lines) corresponding to transitions among terms having multiplicity 4 and 6 and energy lower than about 6eV. These terms are shown in the restricted Fe II Grotrian diagram of fig. 3b. The transition probabilities are those of Kurucz and Peytremann (1975) and of Moore, Minnaert and Houtgast (1966).

As a first approximation the emitting region is supposed to be a spherical, uniform density and temperature cloud with a central source responsible for the excitation. In fig.22 are shown the resulting spectra in the optically thin model.

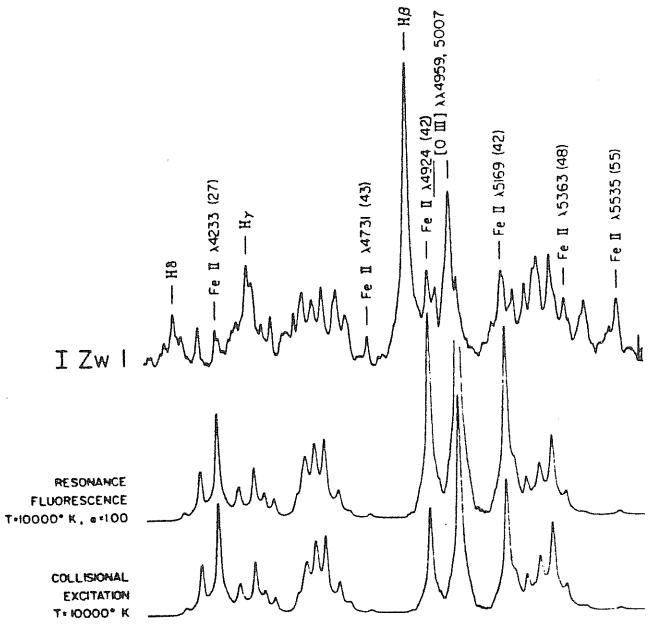

Fig. 22 : the spectrum of I Zw 1 compared with synthetic Fe II spectra of optically thin models.

This hypothesis implies that the line-center optical depth is very low and that the reemitted photons escape the cloud completely. Neither the resonance fluorescence nor the collisional excitation model can match the observations: some lines such as λλ 4924, 4233, 5169 are much stronger than the observed ones while λλ 4731, 5535, although present in the observed spectrum are hardly visible in the synthetic ones. In addition in an optically thin hypothesis the lines belonging to the near-UV multiplets m = 6 and m = 7 should be stronger than the optical lines λλ 4570, 5190 and 5320 that arise from the same upper terms but the observations show a low relative intensity (Phillips, 1977; 1978a). This discrepancy and the similar one observed in the relative intensity of UV 3 and m = 42 (Ulrich et al., 1980) suggests that a large optical depth must exist in the

resonance lines.

To include the optical depth effects in his model calculation, Phillips (1978b) assigns a mean escape probability to each photon emitted in the cloud

$$w(\tau_o) = \sqrt{\pi} \int_{-\infty}^{\infty} \exp(-x^2) \exp[-\tau_o \exp(-x^2)]\, dx$$

With this parameter it is possible to evaluate the probability p_i that a given excitation will eventually result in an observed photon in an emission line. The luminosity in each line is then

$$L_i = h\nu_i p_i C_i$$

where C_i is the excitation rate.

Phillips has subsequently (1978b) modified his early assumption on the geometry of the emitting region: the Fe II lines originate in a large number of homogeneous, optically thick clouds. The optical depth and the velocity dispersion in the absorption lines refer to each single cloud, and the broadening of the emission lines is the result of the relative motions of the clouds. The optically thick resonance fluorescence synthetic spectra are given in fig. 23: the emissions at $\lambda\lambda$ 4924, 4233, 5169 are substantially reduced, because of the increased self-absorption and also the relative intensity of m = 6 and m = 7 (not visible in the figure) match better the observed value. Ther remain, however, the difficulty to produce the observed emissions at $\lambda\lambda$ 4731 , 5535: perhaps some other mechanism

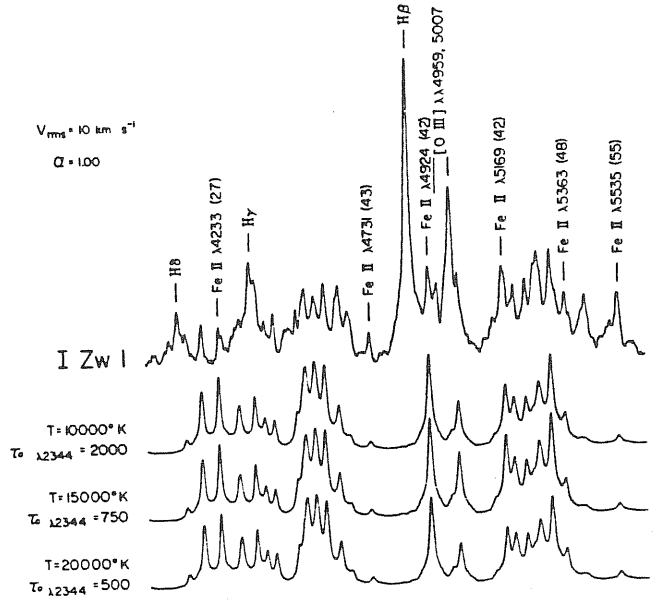

Fig. 23: The spectrum of I Zw 1 compared with the Fe II synthetic spectrum of optically thick resonance fluorescence models.

contributes to these lines too.

In addition, Phillips (1978b) remarks that the synthetic spectra can fit the observations for a wide range of input conditions. In particular the results are quite insensitive to variations in the slope of the continuum and an increment in the temperature tends to produce the same effect as a decrement in the optical depth. The comparison of the observed and the synthetic spectra then, can give only a rough extimation of the physical conditions.

The fit to the observations is not so good in the case of collisional excitation: the best fit is given in fig. 24.

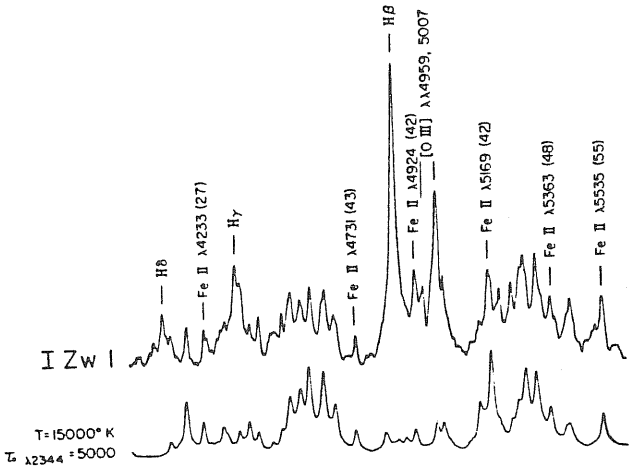

Fig. 24 : the spectrum of I Zw 1 compared with the synthetic Fe II spectrum in the optically thick collisional excitation case.

The blend at λ 4570 is reproduced quite well, and also the emissions at $\lambda\lambda$ 4731 and 5535 show an increased intensity. However, many other lines (see, e.g. $\lambda\lambda$ 4233, 4924, 5363) appear too weak and the emissions observed at $\lambda\lambda$ 5190, 5320 are absent. In addition, the lack of the continuum absorption in the resonance lines, typical of the resonance fluorescence model, is responsible for a number of quite strong emissions in the UV range. Phillips (1978b) estimates that

$$I(\text{Fe II UV})/I(\text{Fe II tot.}) \sim 0.41$$

but, as we have already seen, in many cases there is no evidence for such intense UV emissions (Phillips, 1977; Ulrich et al., 1980; Boksemberg et al., 1978).

Both the resonance fluorescence and the collisional excitation models indicate that the temperature in the emitting region is in

the range

$$10000^{\circ}K < T < 20000^{\circ}K$$

while the optical depth is of the order of 500 - 2000 in the case of fluorescence and much higher ($\tau \sim 5000$) in the second hypothesis.

From the value of τ also the column density of hydrogen, the dimensions and the mass of the emitting region can be estimated:

$$\mathcal{N}(H) \sim \mathcal{N}(Fe^{+}) * \frac{N_H}{N_{Fe}} \frac{N_{Fe}}{N_{Fe^+}}$$

where

$$\mathcal{N}(Fe^{+}) \sim 2 * 10^{13} * \tau \ cm^{-3}$$

(Phillips, 1978b)

$$D \sim \mathcal{N}(H)/N_H$$

$$M \sim N_H * D^3$$

The solar value $N_{Fe} / N_H \sim 3 * 10^{-5}$ is a good approximation while the density of hydrogen and the ionization of iron depend on the assumption on the emission region. If the Fe II lines originate in an H II zone where most of the hydrogen is ionized and most of the iron is in the form Fe^{++}, typical values are

$$N_H \sim N_e \sim 10^{8} \ cm^{-3}$$

and

$$N_{Fe^+}/N_{Fe} \sim 10^{-2}$$

We remark, however, that the absence of Fe II lines suggests that a substantial fraction of iron must be singly ionized.

If the emitting region is a transition (Fe^+, H^o) zone produced by penetrating X-ray photons instead, one can estimate

$$N_H \sim 10 * N_e \sim 10^9 \ cm^{-3}$$

and

$$N_{Fe}/N_{Fe} \sim 1$$

(Phillips, 1978b and ref. therein). The resulting physical parameters are given in table V.

Although the resonance fluorescence model seems to give the best fit, many disturbing problems remain. The evaluated weakness of some Fe II lines, the absence of Si II and Fe III lines in AGN spectra and the impossibility to account for the total emitted energy in the Fe II optical lines unless a complete coverage of the central source by the clouds occurs, are the principal ones.

On the other hand, the collisional excitation model is consistent with the absence of Si II and Fe III lines but gives a worse fit to the Fe II spectrum.

TABLE V

		reson. fluor. ($\delta \sim 2000$)	collis. excit. ($\delta \sim 5000$)
H II zone :	$\mathcal{N}(H)$	$\sim 10^{23}\ cm^{-2}$	$3 * 10^{23}\ cm^{-2}$
	D	$\sim 10^{15}$ cm	$3 * 10^{15}$ cm
	M	$\sim 10^{-4}\ M_\odot$	$3 * 10^{-3}\ M_\odot$
(H^o, Fe^+) :	$\mathcal{N}(H)$	$\sim 10^{21}\ cm^{-2}$	$3 * 10^{21}\ cm^{-2}$
	D	$\sim 10^{12}$ cm	$3 * 10^{12}$ cm
	M	$\sim 10^{-12}\ M_\odot$	$3 * 10^{-11}\ M_\odot$

In addition this mechanism alone can not account as well for the emission in the optical lines (see section III.2 b).

Netzer (1980) suggests that both processes may contribute together and proposes a new calculation of the Fe II synthetic spectrum in a more realistic model for the emitting region, in which the density, the temperature and the ionic abundance are changing across the cloud. He assumes that the Fe II lines originate in a transition (Fe^+, H^o) region, photoionized by a central ultraviolet continuum source. The gas is opaque to the radiation in the Lyman continuum and so most ionization is due to the penetration of soft-X-ray photons. The ionization by the high energy secondary electrons produced when an atom is ionized by an X-ray photon, then, must be included too.

The ionizing continuum is of the form

$$F_\nu \propto \nu^{-\alpha}$$

and the calculations are performed for two values of α. In the first case (case a of Netzer) the usual value $\alpha = 1$ is assumed; in the second model (case b) the presence of a flat continuum permits to test the hypothesis of Netzer and Davidson (1979) that the observed spectrum of quasars is reddened by dust.

As a result of these computations, the values of the electron temperature and density and the ionization of iron are given in each point of the cloud. Netzer then assigns a local escape probability to each Fe II transition, depending on the location of the atom inside the cloud. To simplify the model only the transitions among the terms $a\,^6D$, $a\,^6S$, $a\,^4D$, $a\,^4F$, $z\,^6P^o$ and $z\,^6F^o$ are considered. The probability of re-absorption of a resonance photon is higher in the outer, non-illuminated side of the cloud, where the temperature is lower and the population of the ground terms $a\,^6D$ and $a\,^4F$ is higher. On the other hand, a decrement in the temperature results in a lower population of the metastable term $a\,^6S$ ($E \sim 3$ eV) and a photon of the multiplet $m = 42$ can freely escape on both sides of the cloud. Both resonance fluorescence and collisions are taken into account to excite the atoms, but the calculations show that only a small percentage of the emitted energy in the optical lines is produced by resonance fluorescence. This contribution is never higher than 20% in the case of $m = 42$, but can reach 70% of the emission in the UV multiplets. In fact most of the continuum absorption occurs in the inner illuminated

side of the cloud, where the local escape probability of the UV photons is larger.

TABLE VI

COMPARISON OF OBSERVATIONS AND MODEL CALCULATIONS

LINE	OBSERVED[a]	MODEL a[b]		MODEL b[b]	
		$\tau_{912} = 1.1 \times 10^4$	$\tau_{912} = 3 \times 10^3$	$\tau_{912} = 7 \times 10^4$	$\tau_{912} = 1.8 \times 10^4$
Hβ[c]	1	1 (0.6)	1 (0.7)	1 (0.4)	1 (0.4)
Mg II λ2798	1.6	4.3	2.8	2.1	1.3
C III] λ1909	1.2	4.5	5.8	1.1	1.1
Fe II multiplets:					
42	0.1–0.3	0.1	0.07	0.2	0.14
7F	< 0.05	0.006	0.004	0.03	0.01
UV 2 λ2382	?	0.44	0.65	0.2	0.19
UV 3 λ2345	?	0.15	0.27	0.03	0.05
UV 33 λ2515	?	0.14	0.11	0.08	0.07
UV 34 λ2450	?	0.05	0.06	0.01	0.02
UV 60 λ2950	0.45	0.4	0.35	0.32	0.26
UV 61 λ2875	?	0.1	0.1	0.04	0.05
Σ(42)	...	0.5	0.2	4.5	1.7
Σ(UV 3)	...	395	130	6800	1250
Σ(UV 33)	...	2.4	0.9	34	7.4
Σ(UV 60)	...	7.2	2.9	80	22

[a] Composite spectrum based on Baldwin and Netzer 1978, Grandi and Phillips 1978, 1979, Phillips 1978*a*, and Netzer and Davidson 1979.

[b] The models are shown in Fig. 2. Model *b* includes correction for reddening as described in the text.

[c] Values in parentheses give the line intensity when only recombination is considered.

The principal result of Netzer's calculations are collected in Table VI: the flat continuum model can reproduce better the observed intensities both of the Fe II lines and of other lines such as H β , Mg II λ 2798 and [C III] λ 1909. The ratio Fe II UV/ Fe II opt. is model dependent: the UV lines have comparable intensity to the optical ones for α = 1 but they are about one order of magnitude weaker in the flat continuum case. In addition a possible dependence on the optical depth is suggested. The estimated intensities are such that some UV lines should be detectable in AGN spectra and the author suggests that a strong emission feature at λ 2950, present in many quasar spectra, could be identified with Fe II UV 60. Other broad features at

at $\lambda\lambda$ 2300 - 2600, 2748 and 3200 Å which are observed in many QSOs can all be interpreted as Fe II blended resonance lines (Wills, Netzer, Uomoto and Wills, 1980). Their relative intensities with respect to the Fe II optical lines and to other emission lines are in the range of the predicted values for the flat continuum case.

Although this model is quite succesful in reproducing the gross structure of the observed Fe II spectrum there remain, however, large discrepancies in the detailed shape of individual structures. In particular Wills, Netzer and Wills (1980) identify in the far UV range of some quasars many Fe II emissions from terms at about 8 eV that are too strong with respect to their predicted intensity and Grandi (1981) finds that many observed quasar spectra do not agree with the model calculations. He suggests that many more terms, such as the low lying doublet terms and the terms near 8 eV must be included in the calculation of the synthetic spectrum.

A detailed calculation of the Fe II spectrum including about six hundreds multiplets and two thousands lines is performed by Netzer and Wills (1983). The method of the calculation is similar to that described by Netzer (1980), but the increased number of Fe II transitions suggests that other excitation processes can contribute, together with the collisions, to the emitted spectrum. The authors estimate that if all the optically thick resonance lines of Kurucz's (1981) list are taken into account, assuming a covering factor of 0.1 , a relatively narrow ($V \sim 20 - 40$ Km/sec) absorption profile is sufficient to absorb most of the continuum in the range 2000 - 3000 Å.

The line fluorescence process must be important too, because the

probability of an accidental wavelength coincidence between two lines is strongly increased by the large number of lines. Netzer and Wills (1983) take into account the possibility that line-fluorescence occurs both with the emission lines of other elements and among the Fe II lines themselves and suggest that this last process is the most important in affecting the population of the levels. In a successive work Elitzur and Netzer (1985) consider the possibility that many excitations from the term $a\,^4D$ ($E \sim 1$ eV) could be due to Lyα fluorescence. The introduction of this process in the photoionization model calculation however, does not changes appreciably the Fe II synthetic spectrum. The most evident difference is an increment of about 3 % in the Fe II flux, with most of the energy emitted in a line at about λ 1294 Å. Such a line, however, has never been observed in quasar spectra.

The charge exchange reactions, according to Netzer and Wills (1983), are unimportant because "neither the Fe^{o} nor the Fe^{+} abundance in our model is large enough to explain the observed strength of the high energy Fe II transitions".

The effects of all these mechanisms on the Fe II synthetic spectrum are shown in figs. 25 - 27. In fig. 25 the spectrum calculated without line fluorescence is visible: the most striking feature is the presence of many gaps, around 2100 Å, 2440 Å, 2900 Å and so on..., all of which can be filled by emissions from high energy terms (Grandi, 1981). A much better fit to the observations is instead reached if the line fluorescence mechanism is added. In fig.26 three synthetic spectra for different velocity dispersions

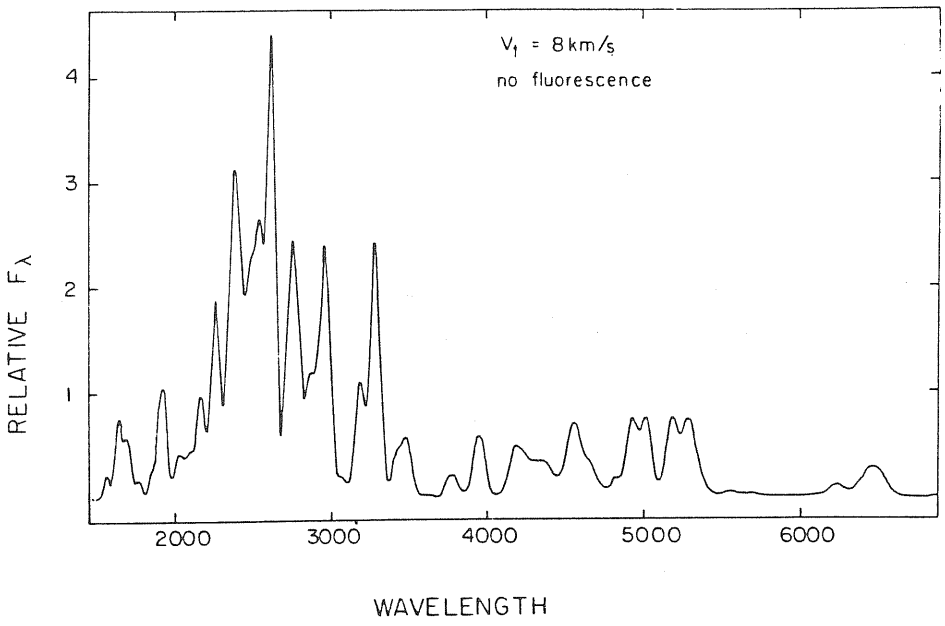

Fig. 25 : the Fe II synthetic spectrum without the line fluorescence contribution.

in the absorption line profiles are given: all the mentioned gaps appear now to be filled. In addition an increasing relative strength of the optical lines with decreasing dispersion velocity is visible. Since for a given photoionization and a thermal absorption profile the dispersion velocity and the optical depth are inversely proportional

$$\sigma(\lambda\ 2343) * V_t = \text{const.}$$

(Netzer and Wills, 1983), a decrease in V_t will result in a higher value of σ and consequentely in a large number of scatterings of the resonance photons. The dependence of the relative ratios of the Fe II lines on the optical depth can be seen even more clearly in

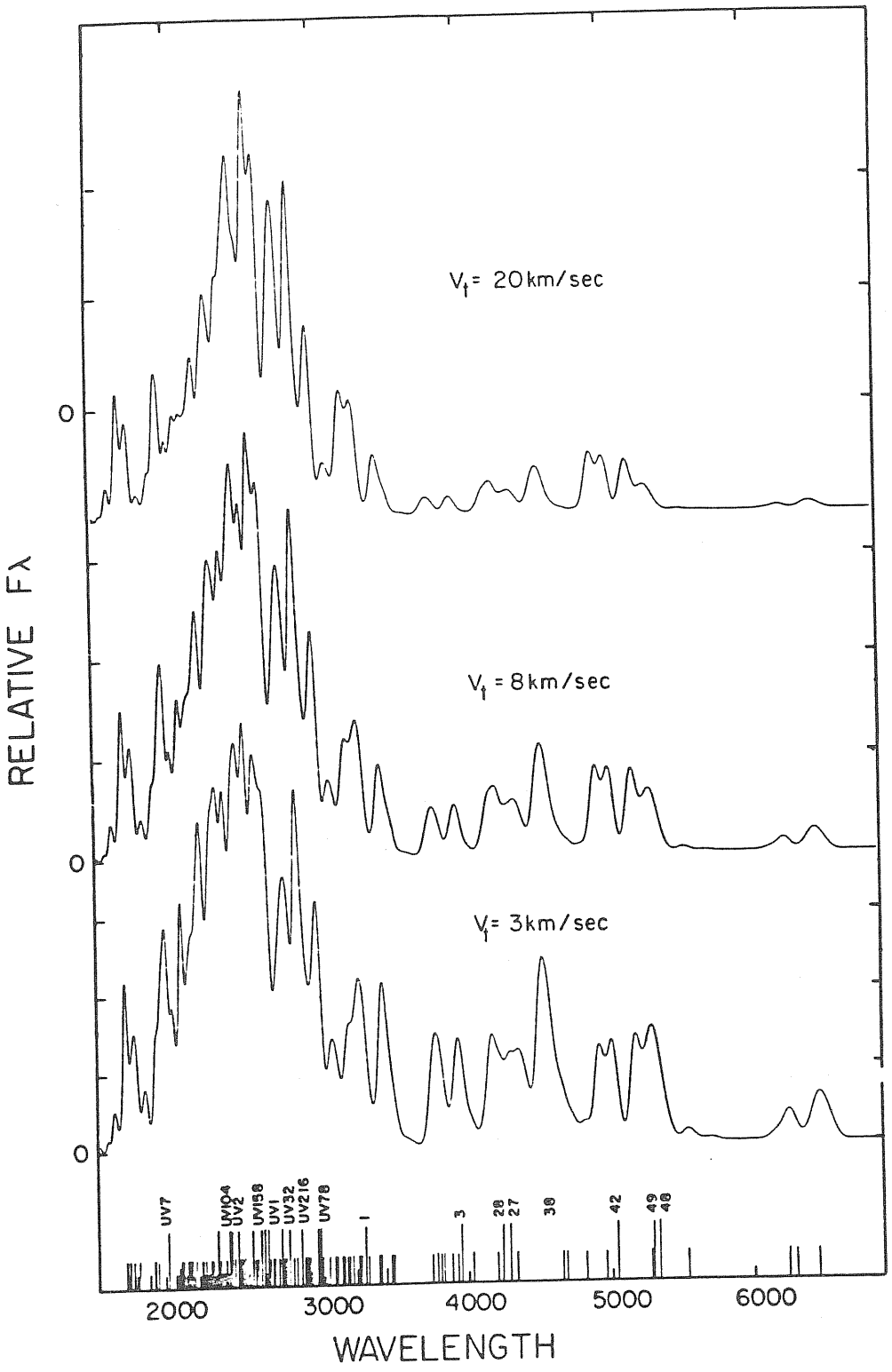

Fig. 26 : different Fe II synthetic spectra with line fluorescence included.

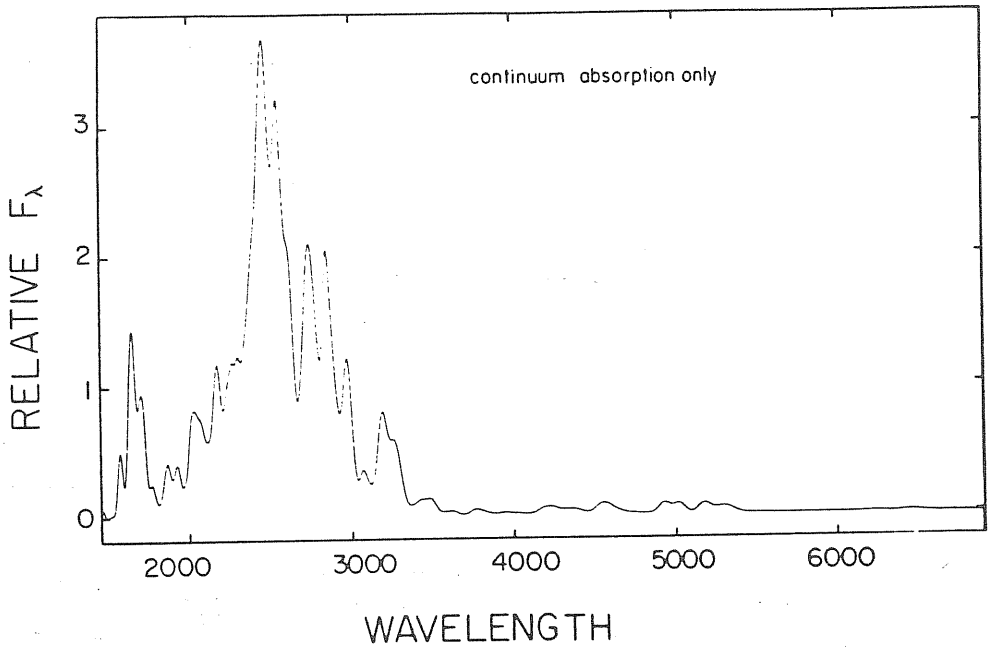

Fig. 27 : the Fe II synthetic spectrum in a pure resonance fluorescence model.

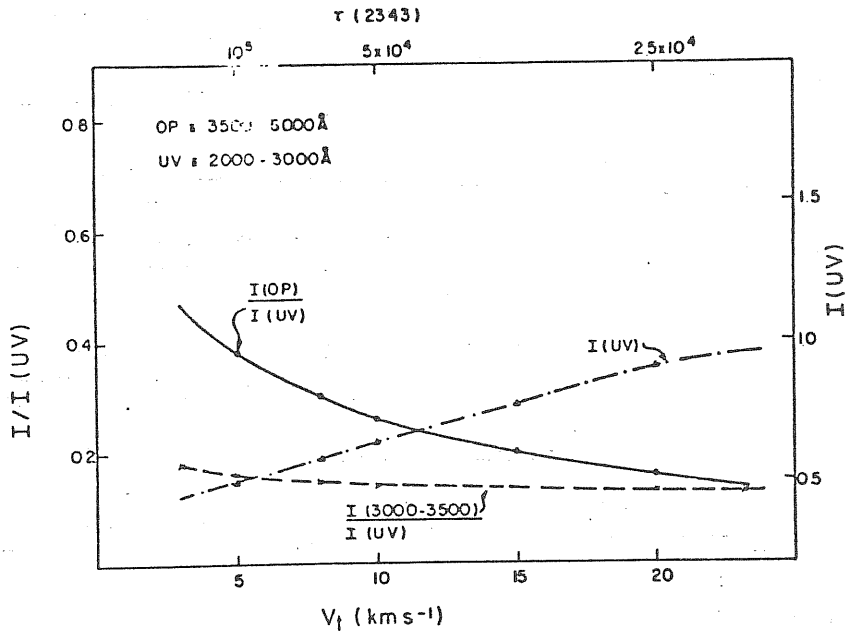

Fig. 28 : the relative intensity of the Fe II emissions versus the optical depth in the resonance lines.

fig. 28. In the same figure the nearly constant ratio of the Fe II UV lines with respect to the multiplets in the range 3000 - 3500 Å is also visible. The near-UV lines can then give some informations on the optical depth in all those cases in which the spectrograms in the UV rest wavelengths are not avaiable.

Finally, the synthetic spectrum calculated in the case in which most of the excitation is due to resonance fluorescence is given in fig. 27. The optical lines appear extremely weak and the fit to the observations is rather poor. This is due to the fact that the photon escape probability is changing across the cloud, as suggested by Netzer (1980). The absorption of the continuum photons occurs preferentially at the illuminated side of the cloud, where the inward escape probability is higher and only a few photons are scattered enougth times to produce the optical lines. This conclusion is opposite to the early consideration (Phillips, 1977) that the continuum fluorescence process should result in strong UV absorption lines. The peculiar structure of the emitting region is not only consistent with the absence of these absorptions , but is also responsible for the quite high UV/opt. ratio of fig. 27.

A quite different result is obtained by Collin-Souffrin et al. (1979). Following the suggestion of Osterbrock (1977) they assume that the emitting region is a finite slab, with constant density and temperature, photoionized by the central source and located at the edge of the H II zone (fig. 29). Since the thickness of the Fe II emitting region is calculated to be small with respect to the dimensions of the BLR, a plane parallel slab is a reasonable approximation. In this geometry however they are forced to assume

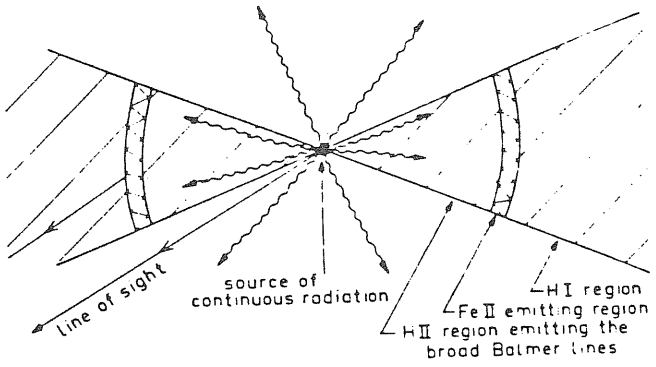

Fig. 29 : a geometrical model for the BLR
in the photoionization case.

a very large turbulent velocity (about 1500 Km/sec) in order to account for the width of the lines. A typical electron density for the Fe II region is

$$n_e \sim 10^{8} \ cm^{-3}$$

and from the time scale of the observed variations in the Balmer lines (Collin-Souffrin et al., 1979 and ref. therein) they evaluate that the distance from the central source (viz. the dimension of the H II zone) is of the order of 10^{17} cm . As a consequence, assuming that the luminosity of the central source is $10^{42} - 10^{43}$ erg/sec, the flux at the slab is

$$L/4\pi R^{2} \sim 10^{7} - 10^{8} \ erg \ sec^{-1} \ cm^{-2}$$

By comparing these values with the limiting values for the occurrence of the various exciting mechanisms (their fig. 2a) they find that AGNs are located in a

transition region where the excitation can be due both to resonance fluorescence and to collisions, in good agreement with the predictions of Phillips (1978b). Recombinations instead appear to be negligible unless a very intense radiation field is present. However, they evaluate that if some radiative process occurs, the Fe II UV lines should appear in absorption in all those cases in which the line of sight of the continuum source crosses the emitting region, but, as already mentiones, no UV absorption line has ever been observed in AGN spectra. A solution can be find if a higher electron temperature ($T \sim 20000\,^{o}K$) occurs in the Fe II region. In fact their computations show that only collisional processes are important in this case. Such a high temperature value, however, can not be the result of photoionization, and the authors are forced to assume a thermal heating for the emitting region.

There is also another reason for rejecting the photoionization hypothesis. The Lyman continuum photons emitted by the central source are absorbed before reaching the Fe II zone, so that neutral iron is ionized by radiation in the range 7.8 - 13. 6 eV, and there are no energetic photons left to ionize Fe^{+} from the ground term (IP~16.1 eV). But if Fe^{+} ions are excited, also photons < 13.6 eV can have enough energy to cause a second ionization. Collin-Souffrin et al. (1979) evaluate that unless charge-exchange reactions are very efficient, most of the iron must be in the form Fe^{++}. Their result, however, does not agree with the observations : Fe II lines are quite common in AGN

spectra, but no Fe III line has ever been observed.

IV.4 The Collisional Ionization Models.

A completely different approach to the problem of the formation of the Fe II lines in AGNs is proposed by Collin-Souffrin et al. (1980). Being aware of the discrepancies with the observations that originate in the photoionization models , they suggest that whatever is the ionizing mechanism in the inner parts of the BLR, the Fe II region is both heated, ionized and excited by collisions. To demonstrate their hypothesis they calculate the synthetic spectrum for a 9-level atom, in the same geometry already discussed by Collin-Souffrin et al. (1979), both in a purely radiative and in a purely collisional case.

In the purely radiative case, that is a photoionized gas excited by continuum fluorescence, they are able to reproduce the observed ratio of the UV/opt. emissions only if a high optical depth in the resonance lines is assumed ($\tau_{UV3} > 5000$). With this high opacity, however, the absolute equivalent widths of the lines are more than one order of magnitude smaller than the observed ones.

The fit to the observations is much better in the purely collisional gas, but it requires a low temperature ($5000^{\circ}K < T < 7500^{\circ}K$), a very high electron density ($n_e \sim 10^{10}$ cm^{-3}) and an even higher optical depth ($\tau_{UV3} \sim 10^{5}$).

With these values the thickness of the shell can be evaluated in the same way described by Phillips (1978b) (see section IV.3). In particular in the collisionally ionized Fe II region the fractional abundance of ionized iron is

$$N(Fe^{+})/N(Fe) \sim 1$$

(Collin-Souffrin et al., 1980) and the calculations give for the slab thickness

$$H \sim 10^{14} \text{ cm}$$

The purely collisional case however is possible only if the emitting gas is shielded from the continuum radiation emitted by the central source. The suggestion of Collin-Souffrin et al. (1980) is that the Fe II emitting region could be located at the periphery of an extended accretion disk, whose inner parts hide the central source. The heating of the gas is then due to the dissipation of turbulent motions produced by instabilities in the disk. From the Shakura and Sunyaev (1973) model they evaluate that if the central object is a black hole of $3 * 10^{8} M_{\odot}$ accreting at its critical rate, a region characterized by

$$T \sim 10^{4} \text{ K}$$

$$n_{e} \sim 10^{12} \text{ cm}^{-3}$$

$$H \sim 10^{14} \text{ cm}$$

must be present at about 10^{17} cm from the black hole. Such a high density however is not consistent with the presence, in many AGNs spectra, of the broad line [C III] λ 1909 that should be collisionally deexcited for $n_{e} > 10^{10} \text{ cm}^{-3}$. The authors are then forced to assume that this line, together with the emission lines

of other highly ionized species, must originate in a different region. A very appealing possibility comes from the presence in the disk of a vertical gradient of the temperature. If the temperature increases outward, as in a chromosphere, then the lines of high ionization, such as [C III] could originate in the outer, lower density zones (fig. 30).

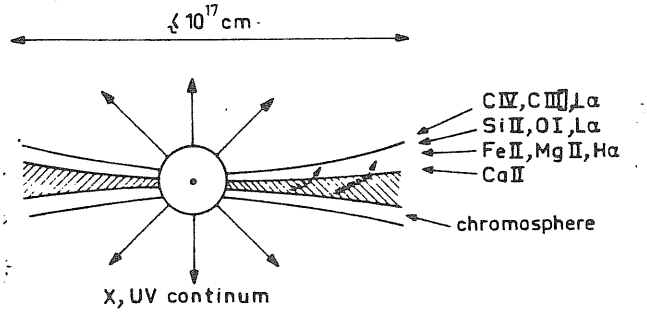

Fig. 30 : the Collin-Souffrin picture for the BLR.

The authors suggest also that the formation of the disk could be linked to the angular momentum of the galaxy, thus explaining the absence of Fe II lines in the elliptical BLRGs and their presence in the spiral Seyfert 1 galaxies. However we point out that some Fe II UV lines have been observed in the BLRG 3C 390.3 (Netzer, Wamsteker, Wills and Wills, 1985) while the Seyfert 2 galaxies, although being spiral galaxies as well, do not show any evidence of these lines.

A successive extension and improvement of this model is due to Joly (1981). She considers a more complete, 14-level atom, in order to account for the recent IUE observations of Seyfert 1 galaxies

and quasars (see section III.1). The assumed framework is the purely collisional case, with an homogeneous emitting shell, shielded from the continuum source and mechanically heated. The role of the charge-exchange reactions on the ionization equilibrium is examined as well. The evaluated intensities for the strongest lines are given in Table VII where they are also compared with the observed emissions in the spectrum of I Zw 1.

TABLE VII

Multiplets	Observed		Computed W_λ						
	I 10^{-13} erg/s cm^2	W_λ	$T_e=10^4$ $n_e=10^{11}$ $\tau_{UV3}\sim 2\,10^5$	$T_e=10^4$ $n_e=10^{12}$ $\tau_{UV3}\sim 10^5$	$T_e=10^4$ $n_e=10^{10}$ $\tau_{UV3}\sim 6\,10^4$	$T_e=10^4$ $n_e=10^{10}$ $\tau_{UV3}\sim 4\,10^5$	$T_e=7500$ $n_e=10^{10}$ $\tau_{UV3}\sim 6\,10^4$	$T_e=7500$ $n_e=10^{10}$ $\tau_{UV3}\sim 4\,10^5$	$T_e=7500$ $n_e=10^9$ $\tau_{UV3}\sim 10^5$
UV 1	1.9	10	8	10	14	14	11	5	9
UV 33	1.6	8	10	11	14	12	8	4	7
UV 34	$\leqq$ 1.2	$\leqq$ 6	7	8	5	4	3	2	2
UV 2 + UV 3 + UV 35 + UV 36	< 3.1	< 15	19	24	19	18	8	6	7
UV 6	1.0	4	5	6	2	1	2	1	1
UV 62 + UV 63 (+ UV 32)	3.2	18	14 (29)	15 (28)	11 (38)	12 (38)	5 (22)	5 (15)	6 (25)
UV 60	2.4	15	13	15	18	16	13	7	11
UV 61	1.4	8	9	11	7	6	5	4	4
4 + 16	1.5	11	20[a]	17[a]	28[a]	28[a]	22[a]	17[a]	23[a]
27 + 28 + (39 + 45)	4.9	45	37 (52)	42 (52)	31 (33)	31 (36)	24 (29)	27 (35)	22 (25)
37 + 38 + 43 (+ 44 + 26)	6.9	70	52 (83)	54 (76)	41 (50)	59 (79)	30 (39)	41 (65)	27 (37)
42 (+ 35 + 36)	2.6	28	16 (46)	19 (39)	11 (31)	9 (61)	16 (29)	13 (42)	12 (28)
48 + 49 + 41	5.1	60	60	60	60	60	60	60	60
46	1.6	20	12	6	[b]	[b]	5	14	8
40	1.3	22	21	16	32	40	38	36	49
Σ UV	17.3	95	105 (120)	117 (130)	118 (145)	111 (137)	77 (94)	51 (61)	70 (89)
Σ Visible	22.4	245	198 (274)	197 (249)	175 (206)	199 (276)	173 (200)	191 (252)	178 (207)

[a] Our Fe II atom does not include multiplet 16, this result concerns only multiplet 4
[b] Multiplet not included in the computation

The intensity of the lines shows a tendency to increase with increasing temperature and optical depth (see also Joly, 1981, figs. 2 ÷ 4), and also the ratio I(Fe II opt.)/I(Fe II UV) increases with γ . This result is in good agreement with that of Netzer and Wills (1983), although a quite different excitation and ionization mechanism has been assumed.

The best fit to the spectrum of I Zw 1 is reached for $T_e \sim 10000$ °K, $n_e \sim 10^{11}$ cm^{-3}, $\gamma_{UV3} \sim 2 * 10^{5}$, but "the other model frame the best fit within a plausible range and owing to the uncertainty on the atomic data, it is difficult to choose among these models".

A similar fit to the spectrum of other Fe II AGNs gives for the physical parameters of the emitting region:

$$7500^{\circ}K \lesssim T_e \lesssim 10000^{\circ}K$$

$$10^{10}\ cm^{-3} \lesssim n_e \lesssim 10^{12}\ cm^{-3}$$

$$\gamma_{UV3} \sim 10^{5}$$

thus confirming the results of Collin-Souffrin et al.(1980).

The physical conditions must instead be quite different in quasars with very weak Fe II optical emissions and intense UV lines (see, e.g. Bergeron and Kunth, 1981; Wills, Netzer and Wills, 1985). In these objects the optical depth must be very low and the emitting region is interpreted as the outer part of a H II region photoionized by the central continuum source (Joly, 1981).

If charge-exchange reactions with hydrogen are introduced in the purely collisional model, they result in an increment of the ratio Fe^{++} / Fe^{+}. The reduced density of singly ionized iron means that a higher column density is needed to obtain the same optical thickness.

Chapter V

The Fe II Spectrum and the Radio Emission.

V.1 The Fe II Emission in radio-loud AGNs.

In the foregoing chapters we have examined the emission mechanisms for the Fe II AGNs , essentially Seyfert 1 galaxies and quasi stellar objects.

This last chapter is instead devoted to the research of a possible explanation for the absence of the Fe II lines in the radio-loud active nuclei.

The BLRGs, although their optical spectra are very similar to those of the Seyfert 1 galaxies, show, on the average, much weaker Fe II lines (Osterbrock, 1982; see also section III.2, fig. 15). The Seyfert 2 galaxies, in whose spectra no evidence of Fe II lines has ever been found, appear to be much stronger radio-emitters than the Seyfert 1 galaxies (see fig. 8). The NLRGs do not show Fe II lines too (Koski, 1978; Costero and Osterbrock, 1977) and, among quasars, most - but not all - of the radio-loud objects have much weaker Fe II optical lines than the radio-quiet quasars. The Fe II emissions in the UV range are instead more common and do not appear to be ralated to the radio-flux (Wilkes and Elvis, 1987 and ref. therein). In fig. 31 the cumulative distribution as a function of the equivalent width of the multiplets m = 37, m = 38 is given for the two classes of quasars (Bergeron and Kunth, 1984).

Miley and Miller (1979) studying the optical spectra of a sample of low-redshift, radio-selected quasars, remark that in all the objects that show detectable Fe II lines, the radio emission does

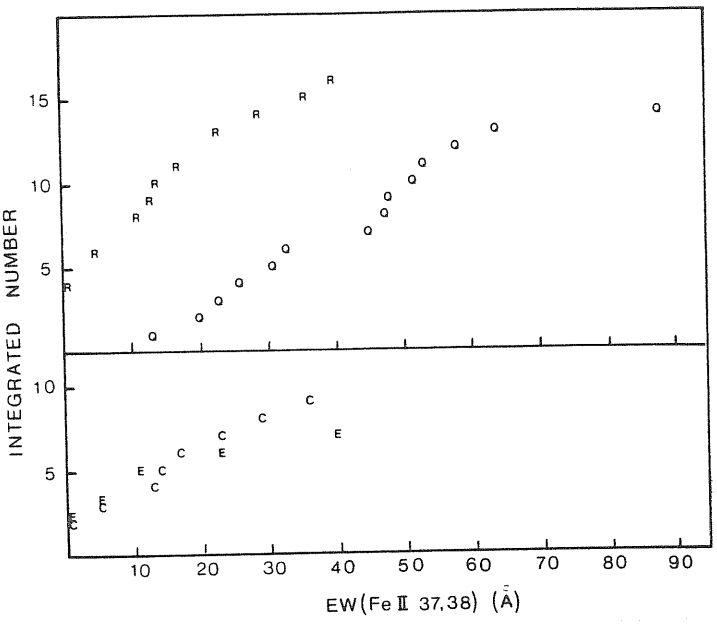

Fig. 31 : above - distribution of radio-loud and radio-quiet quasars according their equivalent width in the Fe II multiplets m = 37, m = 38.
below - the same for compact and extended radio quasars.

not extends more than 50 Kpc from the center. These "compact" quasars are characterized also by relatively narrow and symmetric permitted emission line profiles (fig. 32) and Wills (1982) finds that a unique relation between the intensity in the Fe II optical emissions and the line width probably exists for several classes of AGNs (fig. 33).

All these observations suggest the possibility that the mechanism responsible for the quenching of the Fe II lines must be in some way associated with the radio emission and in particular

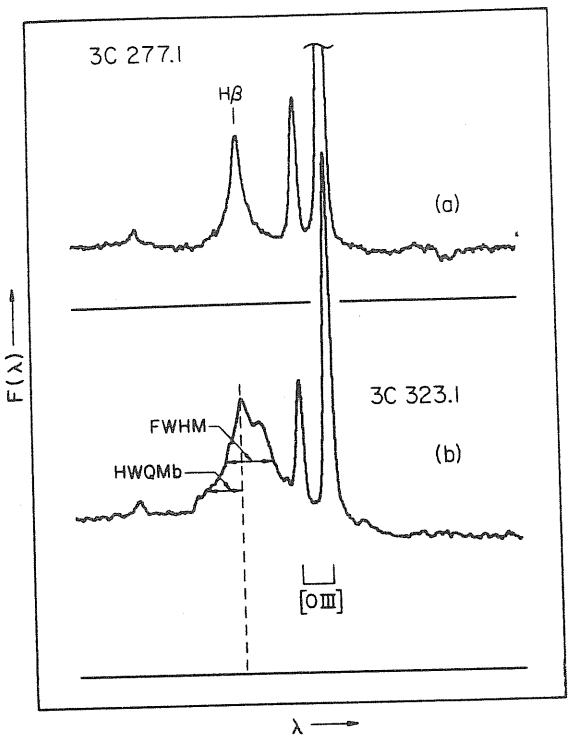

Fig. 32 : the Hβ emission in 3C 277.1 and 3C 323.1: the profile is narrower and more symmetric in the "compact" quasar 3C 277.1.

with the double, extended radio sources.

Various explanations have been proposed: the radio-sources can have too little emitting gas, or the gas can be present at an higher ionization stage (Osterbrock, 1982). The absence of the Fe II lines can reflect an intrinsic difference in the nature of the various classes of AGNs (Heckman, 1983) or be only a consequence of a changing viewing angle (Wills and Browne, 1986). Finally Wilkes and Elvis (1987b) suggest that some other property of the radio-emitting AGNs, such as the X-ray

luminosity, can be the primary factor responsible for the intensities of the Fe II emissions (see also Bergeron and Kunth, 1984).

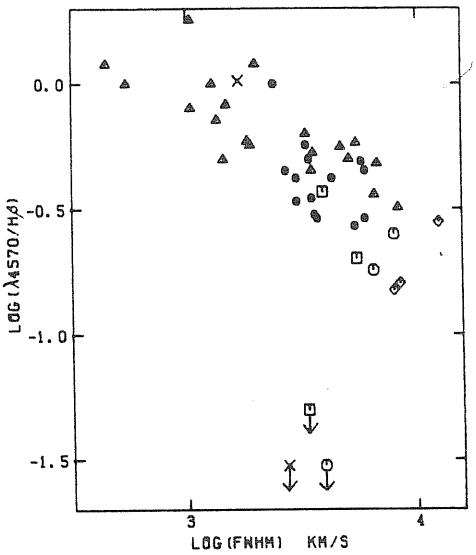

Fig. 33 : the correlation between the relative intensity of Fe II λ 4570 and the width of Hβ for compact quasars (dots), extended quasars (circles), QSOs (crosses), Seyfert 1 galaxies (triangles) and BLRGs (rhombuses).

V.2 The proposed Picture.

Ferland and Mushotzky (1984) point out that in many radio-loud AGNs both the optical and the radio emissions occur on the same distance scale. The size of the radio core is of the order of a few hundreds of parsecs (Ulvestad, Wilson and Sramek, 1981; Miley and Miller, 1979) a value that is comparable with the dimensions of the NLR. Faint, very low-density optical emission regions have been sometimes detected within the extended radio-lobes, at a distance of about 10 Kpc from the centre (Saslaw, Tyson and Crane, 1978; van Breugel et al. 1984). Since the radio-emission is generally assumed to be produced by syncrotron emitting relativistic electrons, such observations indicate that a flow of relativistic particles must be present in the same regions where the line spectrum originates. The authors remark that we do not know if this flow of particles really mixes with the emitting gas but if it is so, the resulting spectrum may be significantly affected. To test their hypothesis they assume that the gas is optically thin to the relativistic electrons and calculate a model in which the interaction with the cosmic-ray is added to the usual photoionization mechanism. The excitation is taken to be due both to resonance fluorescence and to collisions. For simplicity no magnetic field is taken into account although it is necessary for the syncrotron emission, and the only possible interactions between the two components are the two-body collisions. These collisions produce heating losses and ionizations of the atoms of the gas and the authors evaluate that the relative increments in the heating and ionization rates are larger in the transition (H^{o}, Fe^{+}) zone

where the Fe II lines originate. In particular the introduction of the stream of particles decreases the fractional abundance of singly ionized iron and can be the reason for the absence of strong Fe II lines in radio-loud AGNs.

However there are other observational aspects that can not be explained by this picture. If most the iron is mostly in the form Fe^{++} or in an even higher ionization stage, also the UV resonance lines should be strongly affected . These lines are instead quite intense both in BLRGs (Netzer, Wamsteker, Wills and Wills, 1985) and in radio-loud quasars (Wills, Netzer and Wills, 1985). In addition it is not clear why the compact radio sources should have on the average stronger Fe II lines.

A partial explanation in terms of a lower column density can be found if the standard picture holds for these AGNs (Wills, 1982). In the standard picture in fact the compact radio sources are interpreted as the aligned version of the extended, double sources (see also section II.3). The relativistic jets are thought to be viewed end-on and their luminosity are amplified by a factor

$$R \sim D^{2+\alpha}$$

where α is the usual spectral index in the radio wavelength range and D is the Doppler factor

$$D = 1/\gamma \ (1 - \beta \cos \theta)$$

The approaching jet appears then to be the dominant source while very weak large-scale components that could correspond to the extended radio-lobes have sometimes been detected (Browne et al.,

1982; Perley, Fomalont and Johnston, 1982). In such a picture the optically emitting gas is thought to be distributed on a flat configuration perpendicular to the radio axis.

In a core dominant source , because of the small viewing angle the absorbing material is distributed on a very thin layer and this results in a lower number of scatterings and an higher relative intensity of those Fe II lines that have a higher optical depth. Instead, if the source is viewed "edge-on" the increased column density can be responsible for the weakness of the emissions.

However Heckman (1983) points out that this picture can not hold any more in all the intermediate cases, in which the visual is neither parallel nor perpendicular to the radio axis. In fact the radio source appears to be core-dominant only if the angle that the visual makes with the radio axis is very small:

$$\theta \leq 1/\gamma$$

that for $\gamma = 5$ (Orr and Browne, 1982) becomes

$$\theta \leq 10^{\circ}$$

For a larger value the source is lobe-dominant and no Fe II emissions should be seen. It is hard to accept, however, that for $\theta > 10^{\circ}$ the column density has increased to such a high value that the Fe II emissions can not be detected any more.

The problem becomes even more serious if the BLR consists of a spherical distribution of optically thick clouds, as suggested by Netzer (1980), because in such a case no orientation effect can be

invoked. On the basis of these considerations Heckman (1983) concludes that some intrinsic difference responsible for the different Fe II emissions must exist between the compact and the extended radio-sources.

There is another possibility to explain the behaviour of the Fe II lines in the radio-sources, without rejecting the unified model, as proposed by Wills and Browne (1985). They suggest that the principal responsible for the weakening of the Fe II lines in the extended radio-sources is not the optical depth but the increased line width. Indeed the presence of an anti-correlation between the Fe II intensities and the width of Hβ has been pointed out by Wills (1982) (see fig. 33).

By studying the optical spectra of a large number of radio quasars and BLRGs the authors search for a possible correlation between the morfology of the radio source and the width of the lines. The compactness of the source has been quantitatively measured by the ratio R between the intensity of the radio core and that of the extended lobes; the observed correlation between this value and the width of Hβ is given in fig. 34. In the same figure the theoretical relation predicted in the beaming model is also shown. This relation has been evaluated in the assumption that the motion of the emitting gas is confined in the disk plane and that R is related to the angle ϑ that the visual makes with the radio-axis by

$$\cos\vartheta = 1/\beta \; (1/2R \; [2R + R_T - \sqrt{R_T \; (8R + R_T)} \;]\;)^{1/2}$$

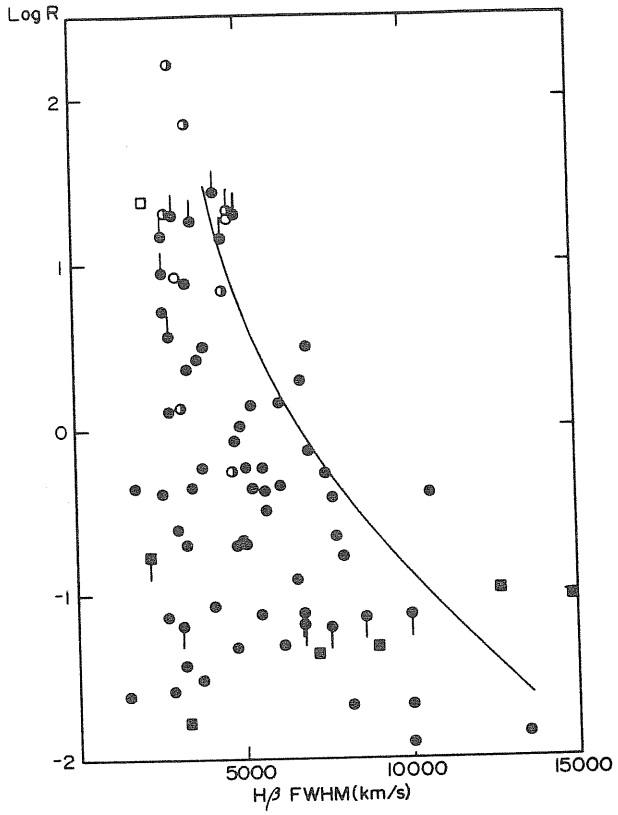

Fig. 34 : the ratio R versus the FWHM of Hβ.

---

where R_T is the value of R for $\theta = 90^0$ (Orr and Browne, 1982).

The data of fig. 34 show that in the extended double radio sources the Hβ and consequently also the Fe II emissions (Phillips, 1977; 1978a) are much broader than in the core-dominant sources, thus confirming the result of Miley and Miller (1979).

Wills and Browne (1985) then suggest that as the Fe II lines become broader, they blend each other and with other weak emissions, to form a pseudo-continuum that can easily be confused with the "true" continuum and that can hide a substantial fraction of the energy emitted in the Fe II lines.

Further optical and UV observations of extended radio sources are needed to test this hypothesis.

V.3 An alternative Explanation.

Another possibility to explain the weakness of the Fe II lines in radio-loud quasars is not directly related to the radio-emission.

Wilkes and Elvis (1987b) point out that the quasi-stellar objects can be classified not only according to their radio luminosity but also to their X-ray properties. Both QSS and QSO are quite strong X-ray emitters (see table II) but on the average the radio-loud quasars are more luminous X-ray sources (Zamorani et al., 1981) and have a flatter soft-X (0.1 - 3.5 KeV) spectrum (Wilkes and Elvis, 1987a). The authors suggest then the X-ray continuum and not the radio emission may be the primary responsible for the intensity of the Fe II lines. They plot the equivalent width of the Fe II emission λ 4570 versus the soft-X-ray spectral index for a sample of 9 low-redshift quasars (fig. 35): a clear trend of increasing equivalent width for increasing slope is visible. However, since the flattest spectra generally correspond to the most luminous radio sources this correlation seem not sufficient to distinguish between the role of the radio and of the soft-X emission in quenching the Fe II lines.

An important indication comes from the presence in the sample of the radio-quiet quasar 1803 + 676. It has the lowest value for the soft-X index and the data show that also the Fe II emissione are

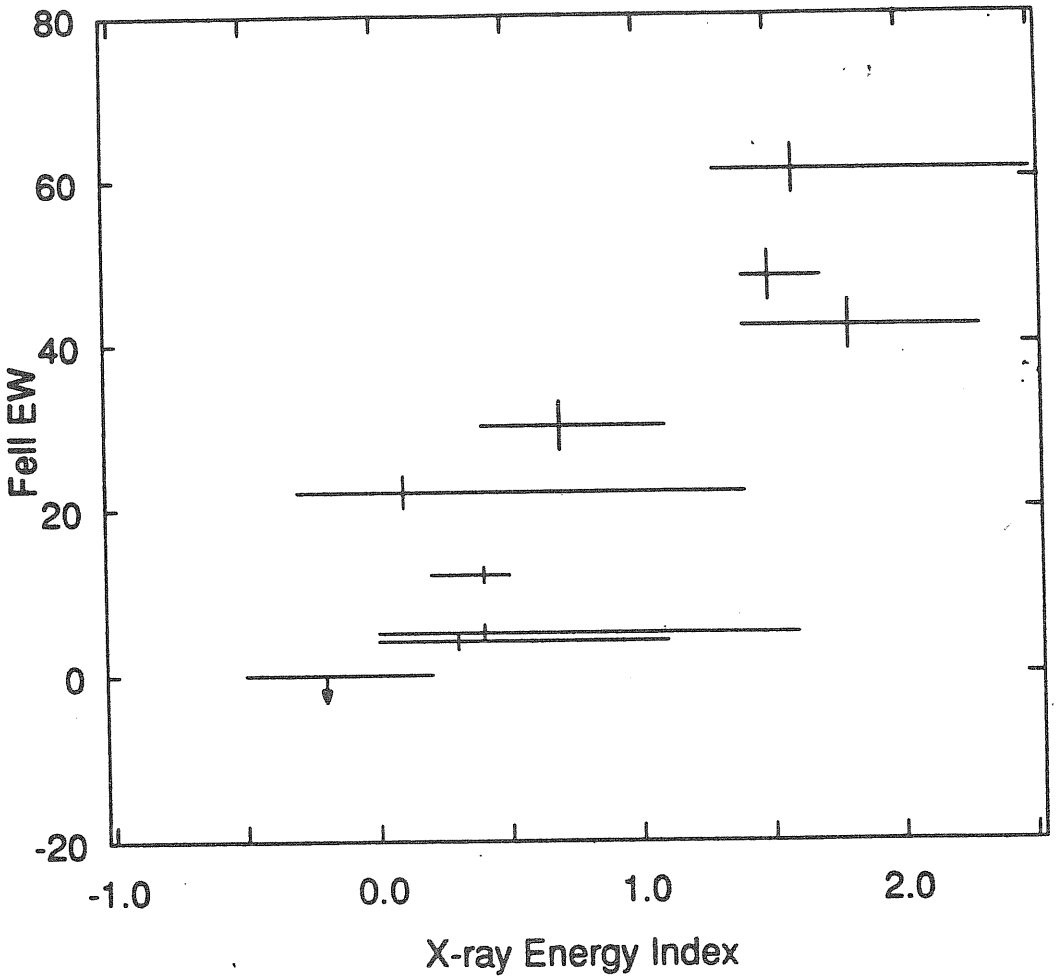

Fig. 35 : the equivalent width of Fe II λ 4570 versus the soft-X spectral index.

---

quite weak, while strong lines are predicted if a correlation with the radio emission exists.

A theoretical argument favouring a correlation between the X-ray continuum and the Fe II emissions comes from the photoionization models for the BLR. In quasars with the flattest spectra a substantial radiation is emitted in the hard-X range (E > 1 KeV).

These energetic photons can deeply penetrate into the BLR clouds and create a warm, partially ionized zone at high optical depth. The Fe II lines , together with other, low-ionization lines, can originate in this region. If this is true, however, the predicted relation should have the opposite trend. If the Fe II lines originate at high optical depth, the UV resonance photons are scattered a large number of times and a high opt./UV ratio is expected.

The authors then suggest that the current photoionization models should be modified to include more realistic X-ray continua and predict that such a modification may reproduce the observed trend (Wilkes and Elvis, 1987b).

This trend is instead consistent with a model proposed by Bergeron and Kunth (1984) in which the BLR clouds are in pressure equilibrium with a hot ($T \sim 10^{7} - 10^{8}$ K) dilute gas responsible for the X-ray emission. In the radio-loud quasars this gas could be hotter than in the radio-quiet, thus explaining the observed excess in the X-ray luminosity and the evaporation time-scale for the "cold" clouds is evaluated to be shorter. The cloud surface density must then be much smaller and this condition implies a lower number of scatterings for the UV resonance photons and much weaker optical lines. It is not clear however, how the gas temperature should be related to the radio luminosity.

V.4 Concluding Remarks.

We have seen that the Fe II emissions are among the most prominent features in various classes of AGNs.

A complete understanding of how these lines are produced is then quite important in order to put light on the nature of active nuclei and to set physical constrains both on the central engine and on the structure of the surrounding region, where the emitted radiation is reprocessed.

The construction of an Fe II synthetic spectrum is highly complicated by the extremely complex structure of this ionic species and by our poor knowledge of the rates of all the physical processes that contribute to excite and ionize the Fe atom. Many models are available in the literature and they indicate a relatively narrow range for the physical parameters of the emitting region, but none of them is able to account for all the observed spectral features. A more sophisticated model of Fe II atom and a more detailed treatment of all possible interactions matter-radiation is requested.

The theory relating the Fe II emissions with the radio emission is not yet satisfactory. Perhaps the emission in the X-ray range and not that at radio-frequencies is the primary responsible for the Fe II spectrum. Further X-ray observations of Fe II AGNs and accurate measurements of the Fe II optical emissions for those quasars having a well-determined X-ray spectrum are needed.

REFERENCES

Antonucci, R.R.J., Miller, J.S.:1985, Ap.J. 297, 621.

Bergeron, J., Kunth, D.: 1980, Astron. Astrophys. 85, L11.

Bergeron, J., Kunth, D.: 1984, M.N.R.A.S. 207, 263.

Boksemberg, A. et al.: 1977, M.N.R.A.S. 178, 451.

Boksemberg, A. et al.: 1978, Nature, 275, 404.

Booler, R.V., Pedlar, A., Davies, R.D.: 1982, M.N.R.A.S. 199, 229.

Brown, A., Ferraz, M.C.de M., Jordan, C.:1984, M.N.R.A.S. 207, 831.

Brown, A., Ferraz, M.C.de M., Jordan, C.:1981, "The Universe at UV Wavelengths. The First two Years of IUE", p.297, ed. Chapman, R., NASA C.P. 2171.

Browne, I.W.A., et al.: 1982, M.N.R.A.S. 198, 673.

Collin-Souffrin, S., Joly, M., Heidmann, N., Dumont, S.: 1979, Astron. Astrophys. 72, 293.

Collin-Souffrin, S., Dumont, S., Heidmann, N., Joly, M.: 1980, Astron. Astrophys. 83, 190.

Condon, J.J.: 1986, Pubbl. A.S.P. 98, 152.

Costero, R., Osterbrock, D.E.: 1977, Ap.J. 211, 675.

Covino, E. et al.: 1986, "Physics of Formation of Fe II Lines outside LTE", IAU Coll. 94, R.Viotti ed.

de Freitas Pacheco, J.A., Landaberry, S.J.C., Lopes, D.F.:1986, Rev. Mex. Astron. Astrofis. 12,185.

de Martino, D., Vittone, A.: 1986, "Physics of Formation of Fe II Lines outside LTE", IAU Coll. 94, R.Viotti ed.

Dere, K.P., Bartoe, J.-D.F., Brueckner, G.E.:1986, Ap. J. 305, 949.

Elitzur, M., Netzer, H.: 1985, Ap.J. 291, 464.

Elvis, M.: 1986, Pubbl. A.S.P. 98, 148.

Engvold, O., Jensen, E., Kjeldseth Moe, O.:1983, Inst. Theor. Astrophys. Oslo. Report No. 59, 65.

Fanti, R., Kellermann, K.I., Setti, G. eds.: 1984, "VLBI and Compact Radio Sources", IAU Symp. 110 (Dordrecht:Reidel).

Ferland, G.J., Mushotzky, R.F.: 1984, Ap.J. 286, 42.

Friedjung, M.:1974, Astrophys. and Space Sci. 29, L5.

Friedjung, M., Malakpur,I.: 1971, Astrophys. Letters 7, 171.

Furenlid, I.:1984, Astron. Astrophys. 140, 49.

Gallagher, J.S., Kenyon, S.J., Hege, E.K.: 1981, Ap.J. 249, 83.

Gahm, G.F.: 1974, Astron. Astrophys. Suppl. 18, 259.

Grandi, S.A.: 1981, Ap.J. 251, 451.

Grandi, S.A., Osterbrock, D.E.: 1978, Ap.J. 220, 783.

Greenstein, J.L., Matthews, T.A.: 1963, Nature 197, 1041.

Gunn, J.E.: 1979 "Active Galactic Nuclei", C. Hazard and S.Mitton eds., Cambridge Univ.

Heckman, T.: 1983, Ap.J. Lett. 271, L5.

Hill, H.G.: 1975, Nature 254, 295.

Hine, R.G., Longair, M.S.: 1979, M.N.R.A.S. 188, 111.

Hubble, E.: 1926, Ap.J. 64, 321.

Hunstead, R.W., Murdoch, H.S., Condon, J.J., Phillips, M.M.: 1984, M.N.R.A.S. 207, 55.

Jaroszynski, M., Abramovicz, M.A., Paczynski, B.: 1980, Acta Astron. 30,1.

Johansson, S.: 1983, M.N.R.A.S. 205, 71P.

Johansson, S.: 1984. Phys. Scripta T8,63.

Johansson, S.: 1986 , "Physics of Formation of Fe II Lines outside LTE", IAU Coll. 94, R. Viotti ed.

Johansson, S., Jordan, C.: 1984, M.N.R.A.S. 210, 239.

Joly, M.: 1981, Astron. Astrophys. 102, 321.

Joly, M.: 1987, Astron. Astrophys. 184, 33.

Jordan, C., Judge, P.: 1984, Phys. Scripta T8, 43.

Koski, A.T.: 1978, Ap.J. 223, 56.

Kurucz, R.L.: 1981, Smithsonian Astrophys. Obs. Special Report 390.

Kurucz, R.L., Peytremann, E. : 1975, Smithsonian Astrophys. Obs. Special Report 362.

Lo,K.Y.: 1986, Pubbl. A.S.P. 98, 179.

MacAlpine, G.M.: 1986, Pubbl. A.S.P. 98, 134.

Marsi, C., Selvelli, P.L.: 1987, Astron. Astrophys. Suppl. 71, 153.

Meyerott, R.E.: 1978, Ap.J. 221, 975.

Merrill, P.W. :1927, Ap. J. 65,286.

Miley, G.K., Miller, J.S.: 1979, Ap.J. Lett. 228, L55.

Moity, J.: 1983, Astron. Astrophys. Suppl. 52, 37.

Moity, J.: 1986, "Physics of Formation of Fe II Lines outside LTE", IAU. Coll. 94, R.Viotti ed.

Moore, C.: 1945, A Multiplet Table of Astrophys. Interest, Revised Edition, Part I

Moore, C.:1952, Atomic Energy Levels, NBS Circ. 467, Vol.I.

Moore, C., Minnaert, M.G.J., Houtgast, J.: 1966, NBS Monogr. 61.

Muratorio, G.: 1985, These de Doctorat, Univ. d' Aix-Marseille.

Muratorio, G., Friedjung,M., Viotti, R.: 1986, IAU Symp. 116, p. 275.

Netzer, H.: 1980, Ap.J. 236, 406.

Netzer, H., Davidson, K.: 1979, M.N.R.A.S. 187, 871.

Netzer, H., Wills, B.J.: 1983, Ap.J. 275, 445.

Netzer, H., Wamsteker, W., Wills, B.J., Wills: 1985, Ap.J. 292, 143.

Nussbaumer, H., Storey,P.J.: 1980, Astron. Astrophys. 89, 308.

O'Dell, S.L.:1986, Pubbl. A.S.P. 98, 140.

Oke, J.B., Lauer, T.R.: 1979, Ap.J. 230, 360.

Oke, J.B., Shields, G.A.: 1976, Ap.J. 207,713.

Orr, M.J.L., Browne, I.W.A.: 1982, M.N.R.A.S. 200, 1067.

Osterbrock,D.E.:1977, Ap.J. 215, 733.

Osterbrock,D.E.:1981, Ap.J. 249, 462.

Osterbrock,D.E.:1982, " Exctragalactic Radio Sources", IAU Symp. 97,D.S. Heeschen and C.M. Wade eds., p.369.

Osterbrock,D.E.:1984, Quart. J. R.A.S. 25, 1.

Osterbrock,D.E.:1987,"Spectroscopy of Astrophys. Plasmas" A.Dalgarno and D.Layzer eds., Cambridge Univ. Press.

Osterbrock, D.E., Koski, T.A., Phillips, M.M.: 1975, Ap.J.Lett. 197, L41.

Osterbrock, D.E., Koski. T.A., Phillips, M.M.: 1976, Ap.J. 206, 898.

Osterbrock,D.E., Shuder, J.M.: 1982, Ap.J.Suppl. 49, 149.

Penston, et al.: 1982, Proceed. of the 3rd Europ. IUE Conf., Madrid, p.69.

Penston, et al.: 1983, M.N.R.A.S. 202, 833.

Perley, R.A., Fomalont, E.B., Johnston, K.J.: 1982, Ap.J.Lett. 255, L93.

Phillips, M.M.: 1977, Ap.J. Suppl. 38, 187.

Phillips, M.M.: 1978a, Ap.J. Suppl. 38, 187.

Phillips, M.M.: 1978b, Ap.J. 226, 736.

Ptak, R., Stoner, R.E.:1973, Ap.J. 185, 121.

Ptak, R., Stoner, R.E.:1976, Ap.J. 210, 25.

Rees, M.J., Begelman, M.C., Blanford, R.D., Phinney,E.S.: 1982, Nature, 295, 17.

Sargent, W.L.W.: 1968, Ap.J.Lett. 152, L31.

Saslaw, W.C., Tyson, J.A., Crane, P.: 1978, Ap.J. 222, 435.

Schmidt, M.: 1963, Nature 197, 1040.

Seaton, M.: 1962, Proc. Phys. Soc. 79, 1105.

Serabyn, E., Lacy, J.H.: 1985, Ap.J. 293, 445.

Seyfert, C.K.: 1943, Ap.J. 97, 28.

Shakura, N.I., Sunyaev, R.A.: 1973, Astron. Astrophys. 24, 337.

Shields, G.A.: 1986, Pubbl. A.S.P. 98, 130.

Shields, G.A., Wheeler, J.C.: 1978, Ap.J. 222, 667.

Smak, J.: 1984, Pubbl. A.S.P. 96, 5.

Steenbock, W.:1985, in "Cool Stars with Excesses of Heavy Elements", Proceed. of the Strasbourg Obs. Coll., Strasbourg, France, 3 - 6 July 1984.

Stein, W.A., Soifer, B.T.: 1983, Ann. Rev. Astron. Astrophys. 21,177.

Stoner, R.E., Ptak, R., Ellis, D.: 1974, Ap.J. 191, 291.

Talavera, A.: 1986, "Physics of Formation of Fe II Lines outside LTE", IAU Coll. 94, R.Viotti, ed.

Tohline, J.E., Osterbrock, D.E.: 1982, Ap.J. Lett. 252, L49.

Ulrich, M.H. et al.: 1980, M.N.R.A.S. 192, 561.

Ulvestad, R.V., Wilson, A.S., Sramek, R.A.: 1981, Ap.J. 247, 419.

van Breugel, W., Heckman, T., Butcher, H., Miley, G.: 1984, Ap.J. 277, 82.

Viotti, R.: 1970, Mem. S.A.It. 41, 513.

Viotti, R.: 1976a, M.N.R.A.S. 177, 617.

Viotti, R.: 1976b, Ap.J. 204, 293.

Wackerling, L.R.: 1970, M.N.R.A.S. 73, 153.

Wampler, E.J., Oke, J.B.: 1967, Ap.J. 148, 695.

Wilkes, B.J., Elvis, M.: 1987a, Ap.J., in press.

Wilkes, B.J., Elvis, M.: 1987b, preprint.

Wills, B.J.: 1982, "Extragalactic Radio Sources", IAU Symp. 97, D.S.Heeschen and C.M. Wade eds. , p. 373.

Wills, B.J., Browne, I.W.A.: 1986, Ap.J. 302, 56.

Wills, B.J., Netzer, H., Uomoto, A.K.,Wills, D.: 1980, Ap.J. 237, 319.

Wills, B.J., Netzer, H., Wills, D.: 1980, Ap.J. Lett. 242, L1.

Wills, B.J., Netzer, H., Wills, D.: 1985, Ap.J. 288, 94.

Zamorani, G. et al: 1981, Ap.J. 245, 357.